STOCHASTIC DOWNSCALING OF CLIMATE MODEL SIMULATIONS FOR SOUTH-WEST WESTERN AUSTRALIA

Bryson C. Bates[1], Stephen P. Charles[1] and Edward P. Campbell[2]

C S I R O

[1]CSIRO Land and Water
[2]CSIRO Mathematical and Information Sciences

Phase 1 report to the

Indian Ocean Climate Initiative

TABLE OF CONTENTS

LIST OF TABLES

LIST OF FIGURES

SUMMARY

During the first year of the Indian Ocean Climate Initiative (IOCI), CSIRO Land and Water (CLW) has examined the utility of stochastic downscaling models for south-west Western Australia (SWA). Downscaling may be defined as the quantification of the relation of local- and regional-scale climate variables to larger scale atmospheric patterns. These patterns may be observed or simulated by dynamical climate models.

Our downscaling experiments have focused on the application of an extended nonhomogeneous hidden Markov model (NHMM) to daily 'winter' (May to October) precipitation across a network of 30 stations scattered throughout SWA. This model was selected on the basis of its documented performance, generality, and ability to cope with small nonstationarity in the atmospheric data. We have addressed the following questions:

1.   Can we downscale observed atmospheric fields?

2.   Are downscaled climate model simulations representative of present day conditions?

3.   Can we validate a downscaling model for changed climate conditions?

4.   What is the potential predictability of downscaled climate model simulations?

Our achievements and preliminary conclusions include:

1.   When fitted to and driven by historical atmospheric circulation data for SWA, the NHMM accurately simulates the wet-day probabilities, the frequency characteristics of dry- and wet-spell lengths, spatial patterns in precipitation occurrence, the daily precipitation amount distributions at each station, and the inter-site correlations for daily precipitation amounts over the 15 year period from 1978 to 1992. This period corresponded to the length of the Bureau of Meteorology's upper air archive when the NHMM was first applied to SWA. Examination of precipitation amount statistics indicates that the NHMM provides a simple and parsimonious method of simulating daily precipitation amounts and their local spatial dependencies across the network. Nevertheless, there is scope for refinement of precipitation amount simulation.

2.   Downscaled simulations from either the CSIRO general circulation model (CSIRO9 GCM) or the CSIRO limited area model (DARLAM) reproduce observed

precipitation probabilities and dry- and wet-spell frequencies at the 30 stations. In contrast, the CSIRO9 and DARLAM simulations of precipitation tend to under-estimate the frequency of dry spells and over-estimate the probability of precipitation and the frequency of wet spells.

3.   The NHMM provides a credible downscaling technique for assessing climate change in SWA provided a variable characterising the closeness of the atmosphere to saturation rather than absolute moisture content is included in its predictor set. The inclusion of this variable (850 hPa dew point temperature depression) was found to be defensible when the NHMM was fitted to either modelled or historical data. Driving the NHMM fitted to historical data with modelled atmospheric fields for changed climate ($2\times CO_2$) conditions results in a small decrease in the probability of precipitation across SWA and a slight change in the region's synoptic climatology. However, this result is based on only one 10-year LAM simulation and is only relevant to the case study region.

4.   Downscaled simulations from an ensemble of four CSIRO9 runs forced by historical sea surface temperatures (SSTs) failed to reproduce the year-to-year variations in 'winter' precipitation for the period 1955 to late 1960s. However, reasonable simulations were obtained for 1970 to 1991. Thus the potential predictability of downscaled GCM simulations was found to be reasonable for this period. Comparison of GCM and historical mean sea level pressure (MSLP) fields suggested that the poor results for the 1950s to 1960s were due largely to errors in the historical SST data rather than the presence of random effects or systematic error in the GCM or the NHMM.

5.   Overall, the above results indicate that CSIRO9 GCM and DARLAM produce credible simulations of atmospheric circulation patterns over SWA. If this were not the case, the statistics of the downscaled simulations would have borne little resemblance to the observed.

Future work will involve:

1.   development of a new NHMM framework that considers precipitation amounts and occurrences jointly;

2.   investigation of the stationarity of NHMM parameters using global MSLP data sets;

3.   driving the NHMM with global MSLP data sets to obtain insight into the long-term, temporal and spatial changes in historical synoptic patterns over SWA;

4.   investigation of the relationship between the changes in synoptic patterns over time and observed secular breaks in SWA precipitation;

5.   a new study of potential predictability using the new NHMM, the Mark 3 version of the CSIRO GCM and an updated historical SST data set; and

6.   for GCM grid cells around SWA, investigation of the interdecadal variability in a 1000 year GCM run with a view to detecting any secular changes in modelled atmospheric series and downscaled precipitation series and identifying their causes.

Outcomes from this work will include:

1.   further insight into the causes and characteristics of the secular breaks in SWA precipitation series at interannual to multidecadal time scales;

2.   assessment of potential climate forecasting skill at local and regional scales;

3.   a new synoptic classification for SWA based on spatial patterns of precipitation occurrence;

4.   insight into climate variation in SWA on time scales ranging from decades to centuries; and

5.   millennial daily precipitation series for climate impacts modelling in SWA.

ACKNOWLEDGMENTS

1.   INTRODUCTION

1.1   Downscaling Climate Model Simulations

Modelling the response of natural and agricultural systems to climate forecasts requires daily data at local and regional scales. The need for improved quantitative precipitation forecasts, and realistic assessments of the regional impacts of natural climate variability and possible climate change due to the enhanced greenhouse effect, has generated increased interest in regional climate simulation. The desire for forecasts based on physical rather than purely statistical models has led to the development of general circulation models (GCMs). Although existing GCMs perform reasonably well in simulating climate with respect to annual or seasonal averages at sub-continental scales, it is widely acknowledged that they do not provide credible simulations of precipitation at the space and time scales relevant to local and regional impact analyses (Arnell *et al.*, 1996). Differences between GCMs, in terms of simulated precipitation and surface air temperature, also seem to be greater at local and regional scales (Gates *et al.*, 1996).

The poor performance of GCMs at local and regional scales has led to the development of limited area models (LAMs) in which a fine computational grid over a limited domain is nested within the coarse grid of a GCM. Grid meshes for LAMs typically range from 20 to 125 km whereas the meshes for GCMs range from 300 to 600 km (Walsh and McGregor, 1995; McGregor, 1997). The host GCM provides the large-scale synoptic forcing to the LAM through the LAM's lateral boundaries. The main advantages of LAMs are that they: allow a more accurate representation of orography; simulate regional climate at a higher spatial resolution than the host GCM; and are more economical to run than a GCM with a similar spatial resolution (Walsh and McGregor, 1995). Nevertheless, LAMs tend to over-estimate the frequency and under-estimate the intensity of daily precipitation and thus do not reproduce the statistics of historical records at the spatial scales of interest in climate impact analyses (e.g., Mearns *et al.*, 1995; Walsh and McGregor, 1995, 1997; Bates *et al.*, 1998). This is due to their inability to resolve the full structure of precipitating systems, the use of parameterisations for other sub-grid scale processes and the propagation of any bias from the coarse-resolution GCM into the LAM simulation.

The above limitations have led to the development of statistical downscaling techniques to derive sub-grid scale weather from the coarse spatial resolution atmospheric data available

from GCMs and LAMs. Early techniques classified large-scale atmospheric circulation patterns, and then modelled the daily precipitation process through multivariate probability distributions conditional on the derived patterns (e.g., Bardossy and Plate, 1991, 1992; Bogardi *et al.*, 1993; Matyasovszky *et al.*, 1993a, b; Bartholy *et al.*, 1995). These schemes produce weather patterns that are defined independently of precipitation and they have had only limited success in reproducing wet and dry spell length statistics (Zorita *et al.*, 1995; Charles *et al.*, 1996). Recent approaches include regressions on continuous atmospheric circulation indices, geographic location and topographical variables (Enke and Spekat, 1997; Huth, 1997; Wilby *et al.*, 1998) and neural networks (e.g., Crane and Hewitson, 1998). However, the success of these methods in simulating the historical process is not always high. For example Enke and Spekat (1997) and Huth (1997) were able to explain only 20% of the at-site variance of historical daily precipitation.

1.2 Nonhomogeneous Hidden Markov Model (NHMM)

The downscaling method described here uses a nonhomogeneous hidden Markov model (NHMM) to simulate precipitation occurrence and multiple linear regression to simulate precipitation amounts in south-west Western Australia (SWA) (Hughes *et al.*, 1999; Charles *et al.*, 1999a). The NHMM relates synoptic-scale, atmospheric circulation variables through a finite number of hidden (unobserved) weather states to multi-site, daily precipitation occurrence data. The NHMM determines the most distinct patterns in a daily multi-site precipitation occurrence record rather than patterns in atmospheric circulation. These patterns are then defined as conditionally dependent on a set of atmospheric predictor variables. Unlike other downscaling techniques based on classification schemes, the weather states are not defined *a priori*. A first-order Markov process defines the daily transitions from weather state to weather state. The process is described as nonhomogeneous as the transition probabilities are conditional on a set of atmospheric circulation predictors. The atmospheric predictors may include raw variables such as mean sea level pressure (MSLP) or derived variables such as north-south MSLP gradient. In this way, the NHMM captures much of the spatial and temporal variability of the precipitation occurrence process. Hughes and Guttorp (1994) show that the NHMM subsumes most existing weather state models.

Model selection involves sequential fitting of several NHMMs with an increasing number of weather states and atmospheric predictors. The fit is evaluated in terms of the physical realism and distinctness of the identified weather states as well as a Bayesian information

criterion (BIC). The objective is to select a NHMM that minimises the BIC, thus identifying a relatively parsimonious model that fits the data well. The most likely weather state sequence is obtained from the selected NHMM using the Viterbi algorithm. This permits the assignment of each day to its respective state (Hughes *et al.*, 1999). The ability to classify days into weather states that are distinct in terms of precipitation as well as synoptic situation means that the realism of the states is directly interpretable in terms of regional hydroclimatology.

The joint distribution of daily precipitation amounts at multiple sites is evaluated through the specification of conditional distributions for each site (Charles *et al.*, 1999a). The conditional distributions consist of regressions of transformed amounts at a given site on precipitation occurrence at neighbouring sites within a set radius. An automatic variable selection procedure is used to identify the neighbouring sites that provide useful information about at-site precipitation amounts. The neighbourhood radius is determined by steadily increasing its size until further increases result in marginal improvements in the proportion of total precipitation variability explained by the precipitation occurrences at neighbouring sites.

1.3 General Circulation and Limited Area Models

We used simulations from the Mark 2 version of the spectral 9-level atmospheric GCM developed by the CSIRO Atmospheric Research (hereafter referred to as CSIRO9 GCM) at horizontal resolutions of R21 (roughly 700 km) and T63 (roughly 300 km). A detailed description of the model can be found in McGregor *et al.* (1993) and thus only a brief outline of its characteristics will be given here. CSIRO9 is intended for general climate simulation and therefore includes the annual and diurnal cycles of sunlight. The model also includes gravity wave drag and computes its own cloud, sea-ice due to thermodynamic effects, soil temperature, soil moisture, and snow cover. Precipitation can be generated by the large-scale circulation and cumulus convection. All land grid-points are assumed to have constant properties except for snow occurrence. Soil moisture content is computed using a two-level scheme whereas three layers are used for computing soil temperatures. A biospheric submodel with 11 plant types and 3 soil types is included. Sea surface temperature (SST) is interpolated daily from monthly data: there is no allowance for diurnal variation of SST. CSIRO9 produces simulations of the present Australian climate that compare favourably with those from models of comparable horizontal resolution (McGregor *et al.*, 1993; Whetton *et al.*, 1996).

We also used 10-year simulations from the limited area model developed by CSIRO Atmospheric Research (CSIRO DARLAM) with a horizontal resolution of 125 km. The simulations consisted of equilibrium (constant atmospheric CO_2 concentration) runs for present day ($1 \times CO_2$) and projected future ($2 \times CO_2$) conditions. Synoptic forcing at the lateral boundaries of the computational grid was provided by CSIRO9 GCM at a horizontal resolution of R21. DARLAM currently uses the same number of vertical levels as the GCM (*Walsh and McGregor,* 1995, 1997).

2. DESCRIPTION OF STUDY AREA AND DATA

We defined SWA as the region extending from about 30° to 35° south and 115° to 120° east (Figure 2.1). The region experiences a 'Mediterranean' climate with abundant winter rains that are nearly double that of any similarly exposed locality in any other continent, and intense summer drought. Eighty percent of annual precipitation falls in the period from May to October, and the majority of winter rains come from low pressure frontal systems (Gentilli, 1972; Wright, 1974). Thus we divided the year into 'winter' (May-October) and 'summer' (November-April) seasons. A full set of 'winter' results are presented in this report.
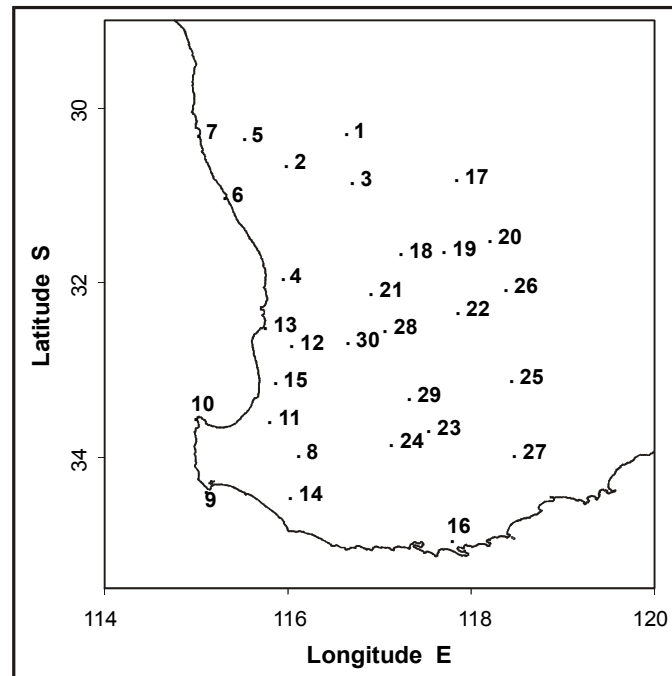
Figure 2.1 Location of daily precipitation stations in south-west Western Australia (for key to numerals see Table 2.1).

Atmospheric data on a Lambert conformal grid were obtained from the Commonwealth Bureau of Meteorology, Australia, for the period from 1978 to 1992. The data at 1100 GMT were chosen on the basis that they are close to the mid-point of the daily precipitation recording period for SWA (24 hours to 0100 GMT, 9 am local time). The available variables included MSLP (hPa) and, at the 850 hPa and 500 hPa levels, geopotential height (GPH, m), air temperature (°K), dew point temperature (°K), and meridional (north-south) and zonal (latitudinal) wind components (knots). Twenty-five variables were derived from this data set. These included the raw variables listed above, the north-south and east-west gradients of the

raw variables, lagged raw variables, and the dew point temperature depression (DTD, °K) at 850 hPa (DTD is the difference between air and dew point temperature). The data for the 25 atmospheric variables were interpolated to a rectangular 3.75° longitudinal by 2.25° latitudinal grid.

Daily precipitation data for 30 stations were obtained from the same data source for the same period. The locations of the stations are shown in Figure 2.1. A key to the numerals shown in Figure 2.1 is given in Table 2.1. These stations were chosen as they had no missing records over this period. The 0, 25, 50, 75 and 100% quantiles for mean annual precipitation are 309 (at station 20), 371, 514, 824, and 1280 mm (at station 12), and for elevation are 2 (at station 7), 102, 252, 293, and 353 m (at station 17). These ranges are representative of conditions in SWA.

We extracted the 1200 GMT fields from the CSIRO9 and DARLAM simulations as these offered the closest synchronisation with the 1100 GMT historical data used to fit the NHMM. The modelled data were interpolated to the grid described above. For all but one of the experiments presented herein, the historical and modelled atmospheric data were centred using their respective means. This removes the effects of any bias in the modelled means on the downscaled simulations. Atmospheric variables derived from the modelled data were used as input to the NHMM: the NHMM was not fit to the GCM or the DARLAM data.

Table 2.1   Details of Daily Precipitation Stations

No. (Fig. 2.1)	Station Name	Station No.	Elevation (m)	Annual Precipitation (mm)
1	Dalwallinu P.O.	008039	335.0	357
2	Moora (Moora Shire)	008091	203.0	461
3	Wongan Hills Res. Stn	008138	305.0	349
4	Perth Airport M.O.	009021	20.0	802
5	Dandaragan (Badgingarra Res. Stn)	009037	260.0	598
6	Lancelin	009114	4.0	627
7	Jurien	009131	2.0	560
8	Bridgetown P.O.	009510	150.0	843
9	Augusta (Cape Leeuwin A.W.S.)	009518	14.0	1000
10	Busselton (Cape Naturaliste L.H.)	009519	97.0	830
11	Donnybrook P.O.	009534	63.0	1002
12	Dwellingup (Forestry)	009538	267.0	1279
13	Mandurah (Park)	009572	15.0	888
14	Pemberton (Forestry)	009592	174.0	1213
15	Harvey (Wokalup Agric. Res. Stn)	009642	116.0	996
16	Albany A.M.O.	009741	68.0	805
17	Bencubbin (Bencubbin)	010007	353.0	320
18	Cunderdin P.O.	010035	236.0	368
19	Kellerberrin (composite)	010073	247.0	333
20	Merredin (Res. Stn)	010093	318.0	309
21	Beverley P.O.	010515	199.0	422
22	Corrigin P.O.	010536	295.0	378
23	Katanning P.O.	010579	310.0	485
24	Kojonup (composite)	010582	305.0	542
25	Lake Grace P.O.	010592	286.0	353
26	Narembeen P.O.	010612	276.0	332
27	Ongerup (Ongerup)	010622	286.0	383
28	Pingelly P.O.	010626	297.0	455
29	Wagin P.O.	010647	256.0	440
30	Wandering (Shire)	010648	280.0	626

3.   CAN WE DOWNSCALE OBSERVED ATMOSPHERIC FIELDS?

3.1   Introduction

In an earlier study (Hughes *et al*., 1999), a split sample validation using historical atmospheric and precipitation data showed that a 6-state NHMM with three atmospheric predictors (the mean of MSLP across five grid points (hereafter referred to as mean MSLP), north-south MSLP gradient, and east-west gradient in GPH at 850 hPa) could provide credible reproductions of at-site precipitation occurrence probabilities and their spatial association, and dry- and wet-spell length statistics for the gauges listed in Table 2.1. (A dry spell is defined as a sequence of consecutive days during which daily precipitation remains below 0.3 mm. A wet spell is defined as a sequence of consecutive days during which daily precipitation equals or exceeds 0.3 mm.) The validation involved fitting the NHMM to data for the period from 1978 to 1987, and testing the model using the reserved data for 1988 to 1992. Increased variability in the NHMM simulations was found when the model was applied to the reserved data but no systematic biases were evident. This is important as a small but measurable shift in the atmospheric variables occurred in the 5-year reserved data period compared with the 10-year period used for NHMM fitting (-0.81 hPa in MSLP, 0.47 hPa in north-south MSLP gradient, and 0.45 m in east-west gradient in GPH at 850 hPa). Thus the NHMM was able to adjust the precipitation occurrence probabilities to account for slight nonstationarity in the atmospheric data.

Subsequent work showed that a noticeable improvement in the BIC criterion could be obtained if the east-west gradient in GPH at 850 hPa was replaced by DTD at 850 hPa (Charles *et al.,* 1999a,b). The new predictor was found to be preferable to dew point temperature at 850 hPa. Although the latter is a proxy for the absolute moisture content of the lower atmosphere, it can be argued on physical grounds that the probability of precipitation occurrence would be better related to a measure of saturation and hence the probability of cloud formation, such as DTD.

3.2   Approach

In the following section we present diagnostic plots for the 6-state NHMM with MSLP, north-south MSLP gradient, and DTD at 850 hPa as atmospheric predictors. These plots facilitate assessment of the NHMM's ability to reproduce observed precipitation statistics that are not incorporated directly into the model. For the precipitation amounts module, a 300 km

radius was used to define the neighbourhood around each station. This radius provided a reasonable trade-off between model parsimony and explained variance (Charles *et al.,* 1999a). Ten 15-year sequences of daily precipitation were generated from the NHMM, conditionally on the 15-year sequence of historical atmospheric data.

3.3   Results

Figure 3.1 shows the precipitation occurrence probability patterns and the corresponding composite MSLP fields associated with the six weather states. The weather states are reasonably distinct and have a high degree of physical realism in terms of the synoptic situation, their relative frequency and associated precipitation amounts (Table 3.1).
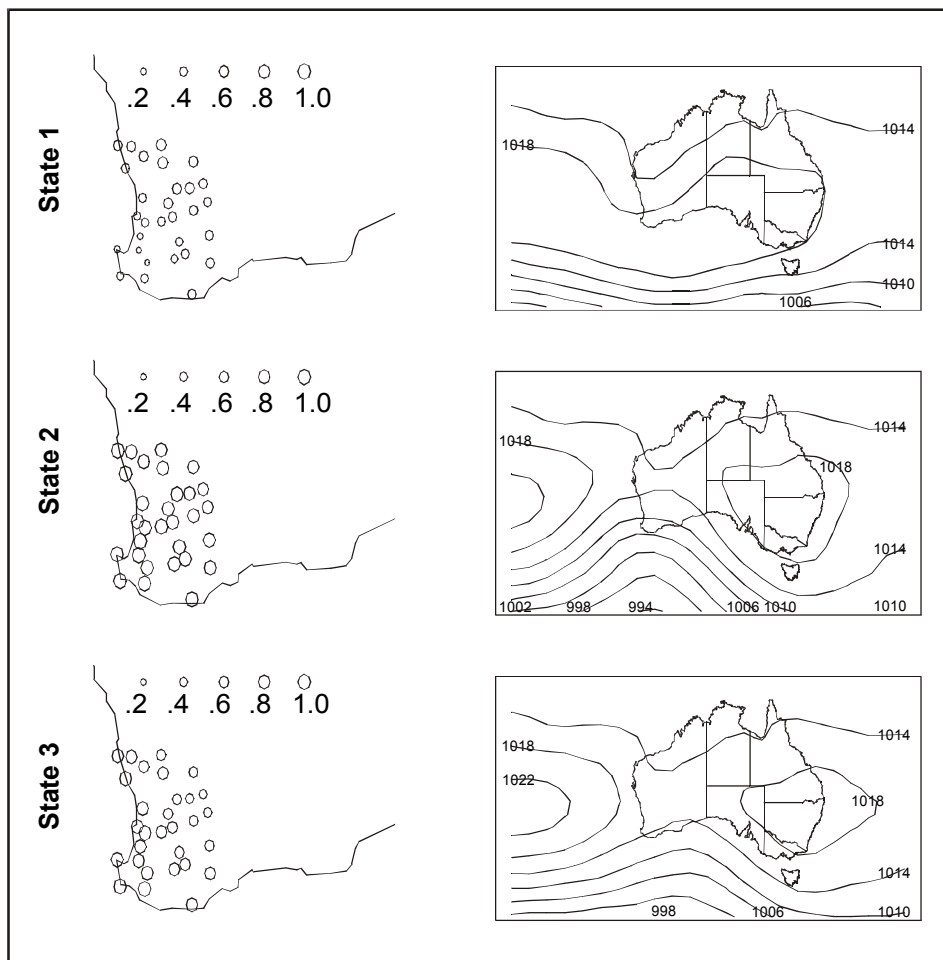
Figure 3.1 (a)   'Winter' precipitation occurrence patterns and MSLP averaged over all days classified under each weather state for the selected NHMM.
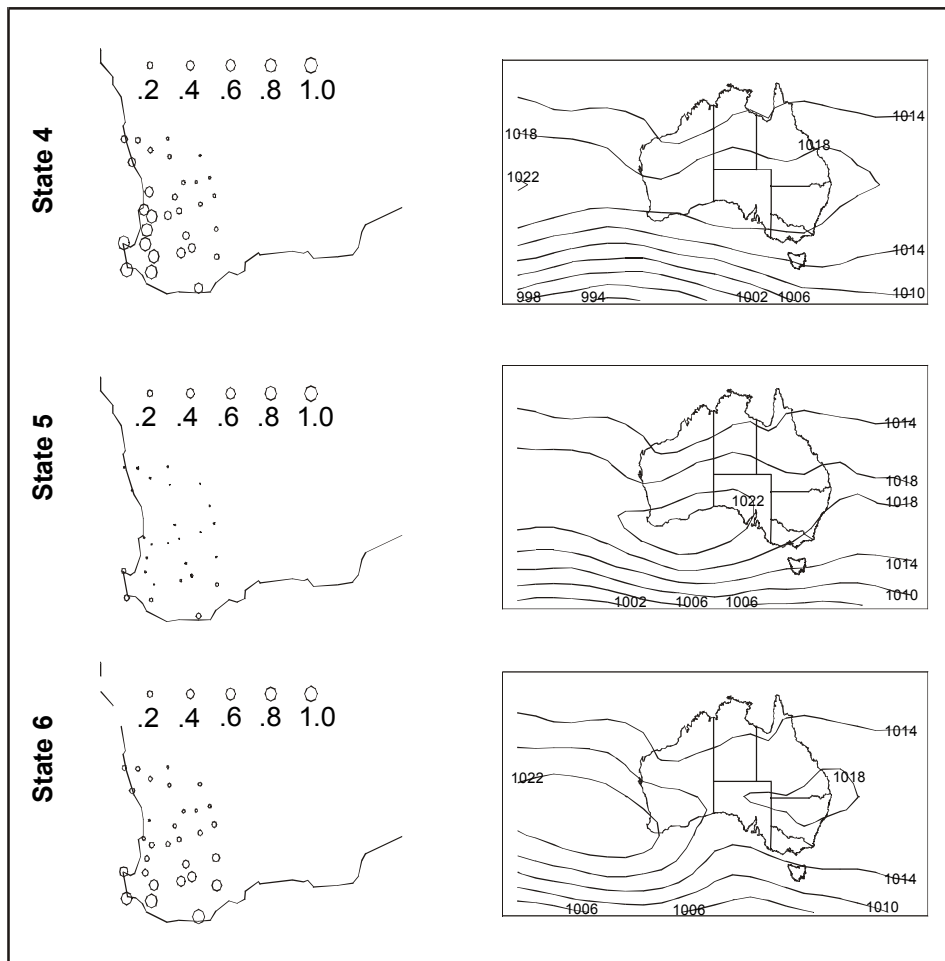
Figure 3.1 (b)   'Winter' precipitation occurrence patterns and MSLP averaged over all days classified under each weather state for the selected NHMM.

Figure 3.2 compares the simulated daily precipitation occurrence probabilities with historical values for the 30 stations. The simulated precipitation probabilities are close to the observed across all stations.
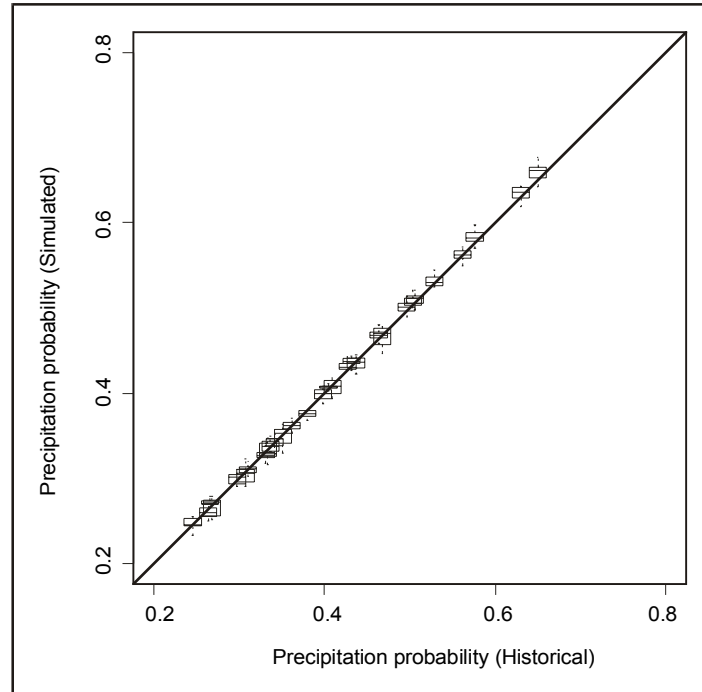
Figure 3.2   Historical versus simulated probability of 'winter' daily precipitation. The edges of the boxes mark the upper and lower quartiles of the ensemble. The horizontal line within each box denotes the median, and the end points of the whiskers attached to each box denote the simulated extremes

Figure 3.3 compares the historical distributions and mean simulated distributions of dry-spell lengths at six representative stations spread across SWA. The mean simulated distributions provide good approximations to the historical distributions, particularly for the short duration spells that encompass about 90% of dry events. The discrepancies for the remaining 10% of events may be attributable to uncertainty in their probability estimates due to the small sample sizes involved. Also, the tendency to underestimate the lengths of extreme dry spells is exaggerated by the use of a log probability scale.
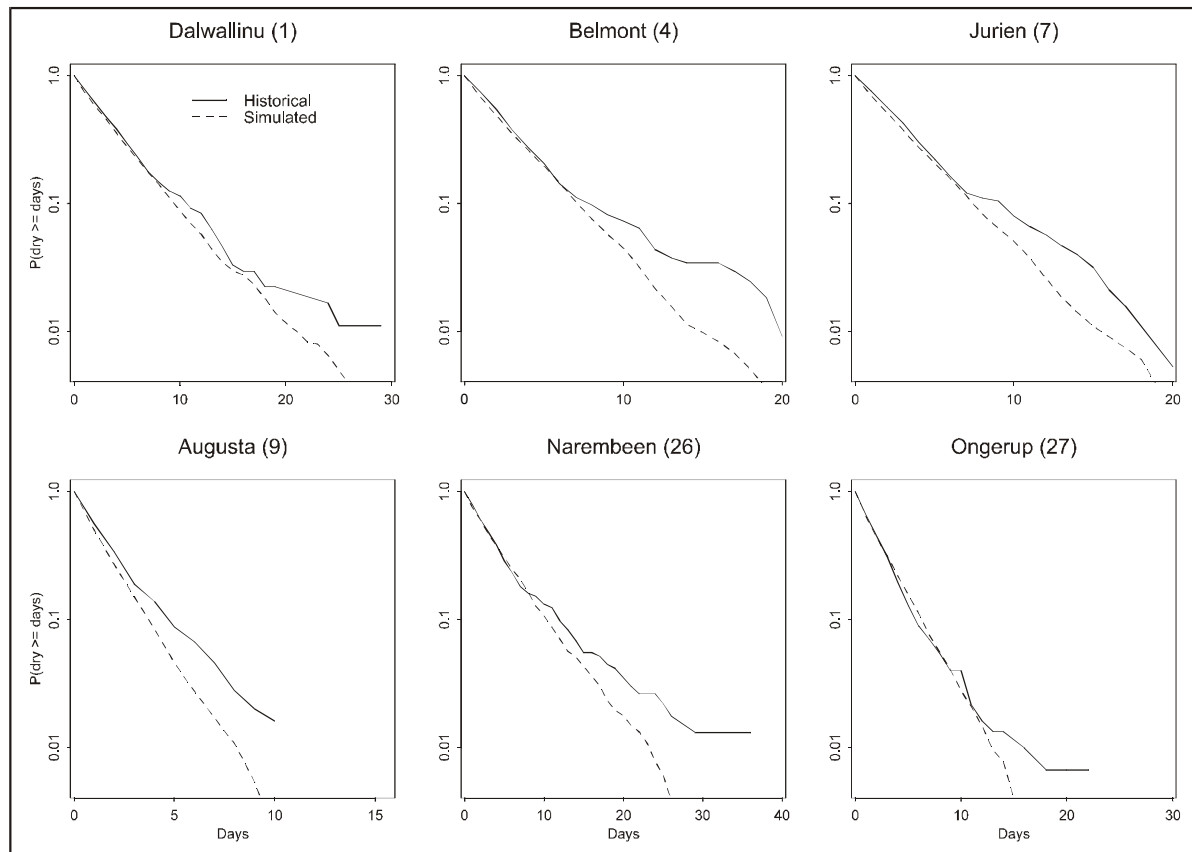
Figure 3.3   **Comparison of historical and mean simulated dry spell length distributions for eight stations in SWA. (The locations of the stations are shown in Figure 2.1)**

Table 3.1   Summary of Weather States

State No.	Description of Synoptic Situation	No. of Days (%)	Rainfall (%)*
1	Trough in the easterlies over SWA.	6.5	7.8
2	Trough in the westerlies over SWA.	19.8	65.9
3	Ridge to north of SWA and trough to east; generally west to south-west airflow.	14.1	16.4
4	Ridge across north of SWA; generally west to north-west airflow south of ridge.	20.2	6.9
5	High centred east of SWA; generally east to north-east airflow.	27.8	0.5
6	High centred west of SWA; generally south-west to south-east airflow.	11.6	2.5

* Percentage of mean winter rainfall (average of the 30 stations shown in Figure 2.1).

Figure 3.4 compares the historical distributions and the mean simulated distributions for wet spell lengths at six representative stations. The mean simulated distributions provide good approximations to the historical distributions, particularly for the short duration spells that encompass approximately 99% of wet events.
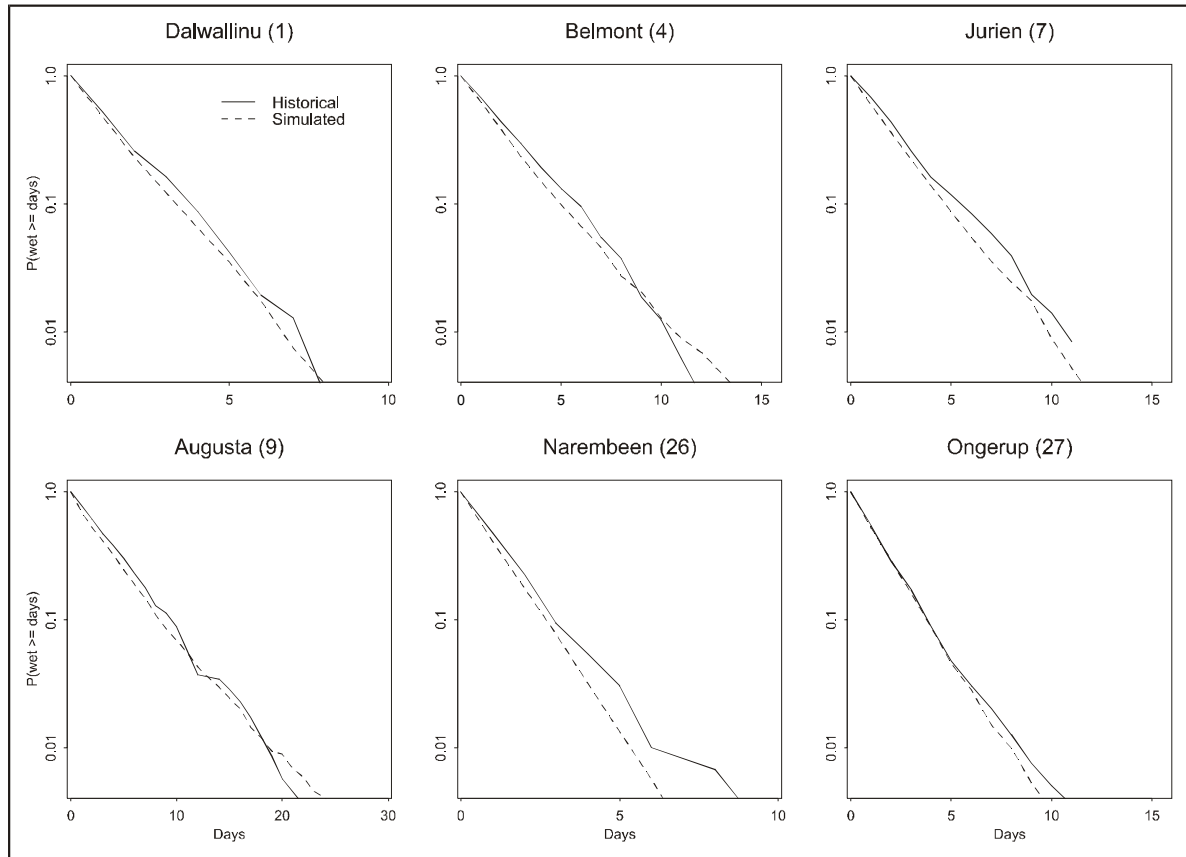
Figure 3.4 **Comparison of historical and mean simulated wet spell length distributions for eight stations in SWA. (The locations of the stations are shown in Figure 2.1)**

Figure 3.5 compares the mean simulated log-odds ratio for precipitation occurrence with the observed. (The log-odds ratio is a measure of association for binary data that is analogous to spatial correlation of continuous variables [Kotz and Johnson, 1985]) The selected NHMM clearly captures the spatial correlation between stations that is induced by the weather states and other effects such as local orography and aspect.
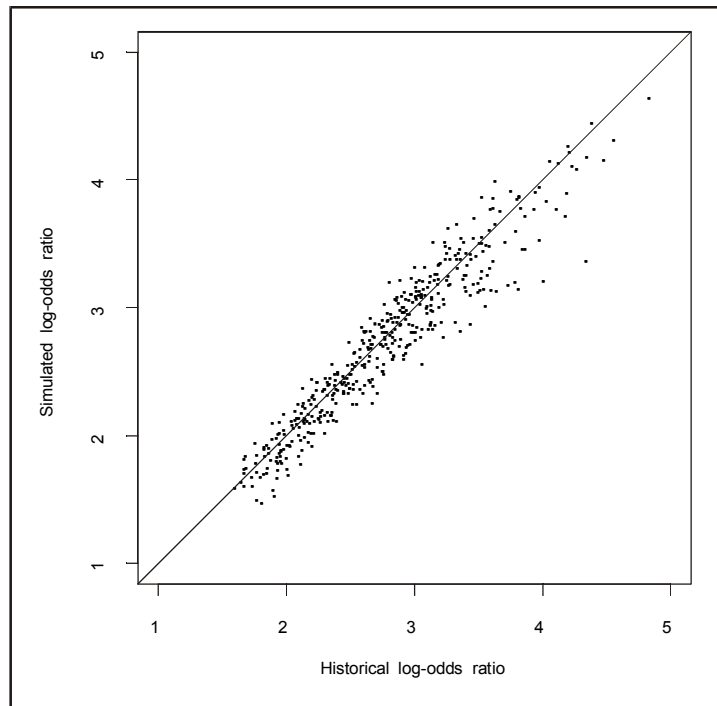
Figure 3.5   Historical versus mean simulated log-odds ratio

Figure 3.6 compares the distributions of the historical and simulated precipitation amounts at six representative stations, for one of the ten generated sequences chosen at random. Some discrepancies in the upper tails of the distributions are evident due to deficiencies in simulating amounts for days in weather state 2. In state 2, all stations are likely to be wet so there is little information on amounts in the precipitation occurrence pattern for this state (Figure 3.1 and Table 3.1). However, the model does well in reproducing all but the largest quantiles of at-site precipitation.
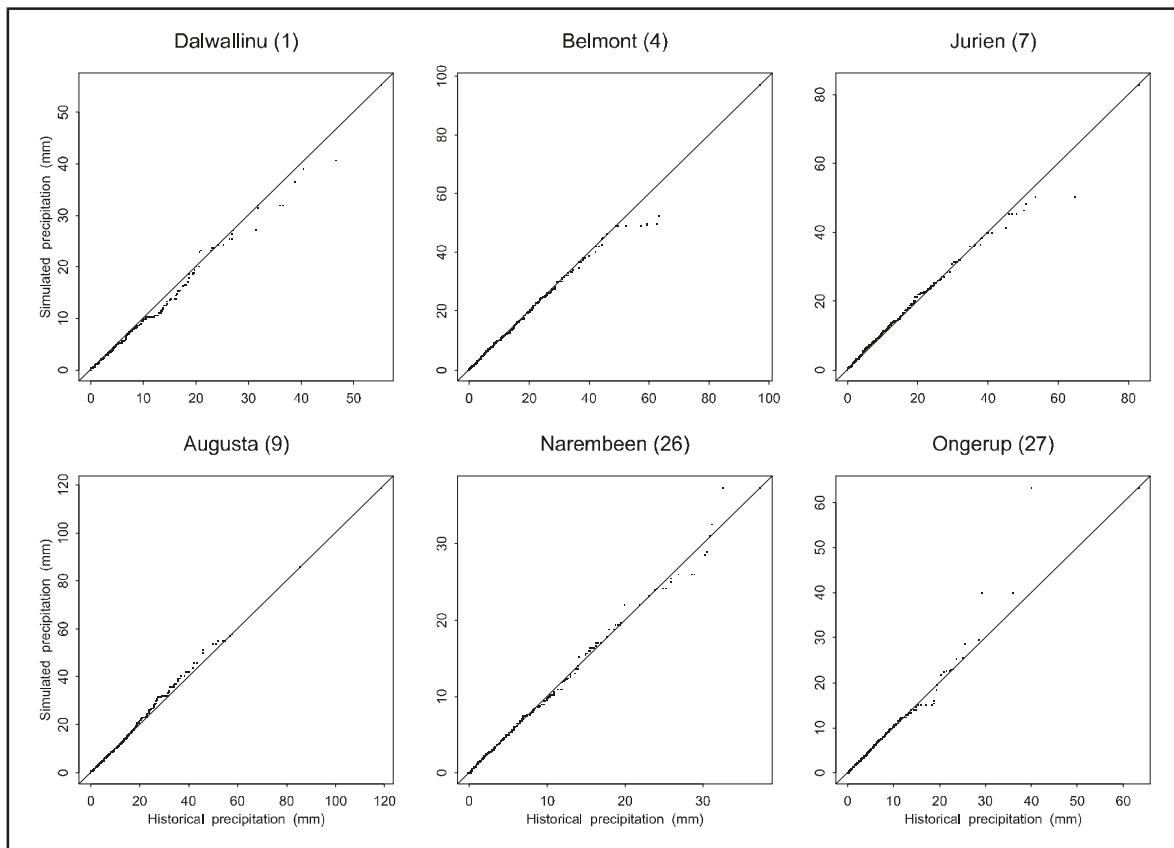
Figure 3.6   Quantile-quantile plots of historical versus simulated precipitation amounts for six stations in SWA. (The locations of the sites are shown in Figure 2.1)

Figure 3.7 compares the historical versus simulated Spearman rank intersite correlations for the generated sequence. The Spearman rank correlation coefficient is a measure of association between two variables that is not subject to assumptions about the form of the underlying population distribution. In contrast, the conventional correlation coefficient assumes that the joint distribution of the variables is bivariate normal. There is a bias of -0.03 in the simulated correlations across the range of historical correlations. Increasing the neighbourhood radius failed to produce a noticeable reduction in the bias. The remaining nine generated sequences produced similar results.
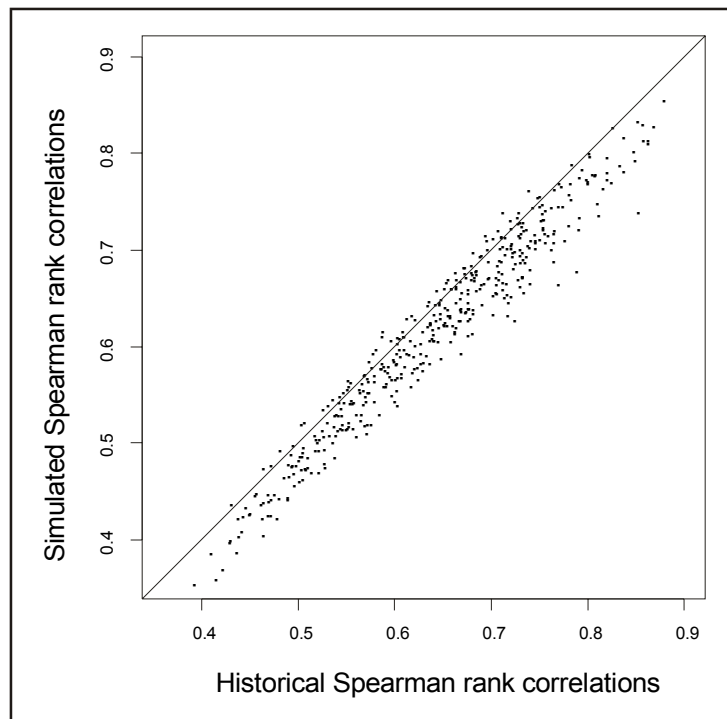
Figure 3.7 **Historical versus simulated Spearman rank intersite correlations**

4.   ARE DOWNSCALED CLIMATE MODEL SIMULATIONS REPRESENTATIVE OF PRESENT DAY CONDITIONS?

4.1   Introduction

A common approach to greenhouse science experiments is to carry out a set of climate model runs for equilibrium conditions. These runs typically cover present day ($1\times CO_2$) conditions and projected future ($2\times CO_2$, $3\times CO_2$, etc.) conditions. Using atmospheric fields from equilibrium GCM and LAM runs for present day conditions to drive a downscaling model that has been successfully fitted to historical data provides an independent test of the veracity of the simulated large-scale atmospheric circulation patterns. It also provides a means of assessing whether the downscaled precipitation statistics are representative of observations.

4.2   Approach

Bates *et al.* (1998, 1999) showed that DARLAM and CSIRO9 simulations tend to under-estimate the frequency of dry spells and over-estimate the probability of precipitation and the frequency of wet spells. In this section, we examine the ability of downscaled DARLAM and CSIRO9 runs to reproduce observed rainfall frequencies, storm durations and storm interarrival times at the 30 stations depicted in Figure 2.1.

4.3 Results

Figure 4.1 compares the downscaled daily 'winter' precipitation occurrence probabilities with historical values for the 30 stations. The downscaled precipitation probabilities for both CSIRO9 and DARLAM are close to the observed across all stations.
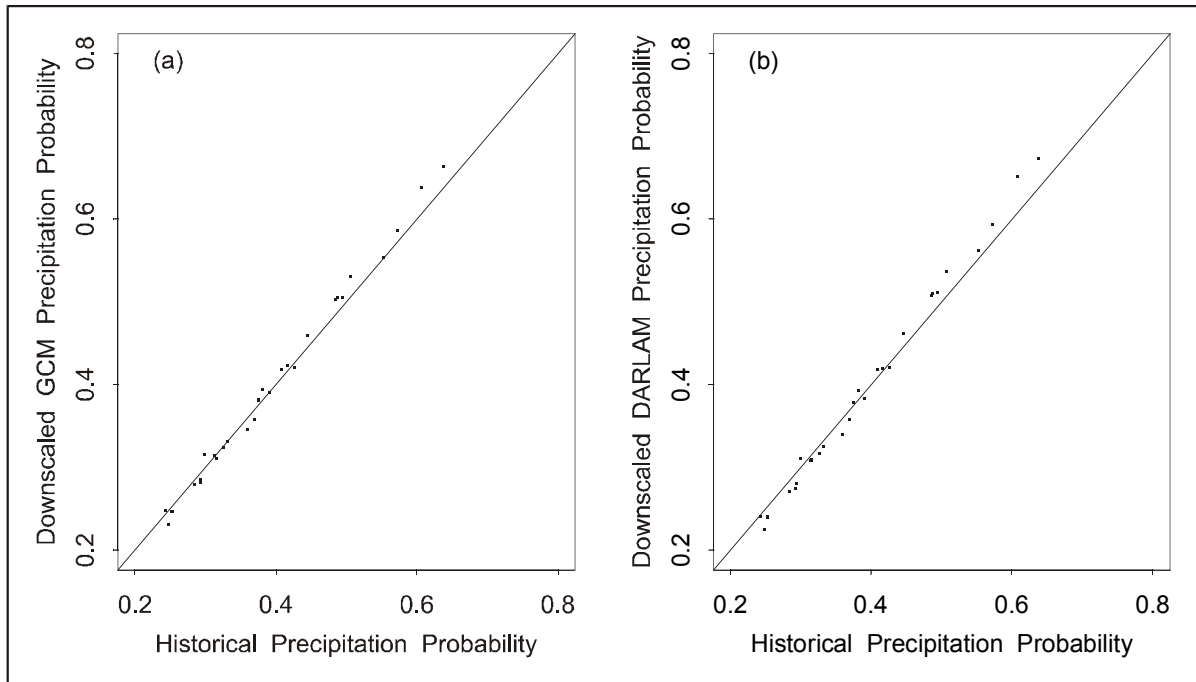
Figure 4.1   Comparison of downscaled and historical daily 'winter' precipitation occurrence probabilities

Figure 4.2 compares the historical distributions and the downscaled distributions for dry spell lengths at 8 of the 30 stations. The downscaled distributions provide good approximations to the historical distributions, particularly for the short duration spells that encompass approximately 90% of dry events. Moreover, there are only slight differences in the downscaled distributions obtained from CSIRO9 and DARLAM.
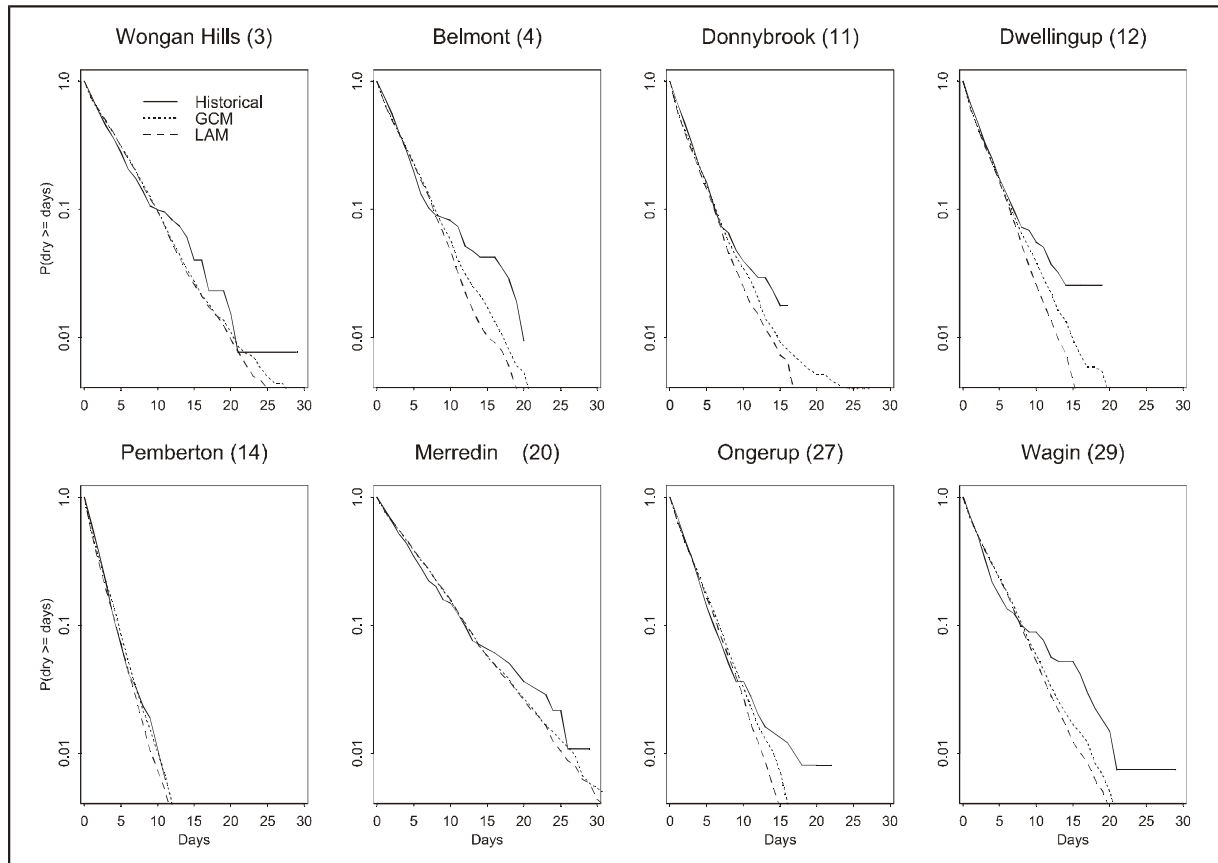
Figure 4.2   Comparison of historical and downscaled dry spell length distributions for eight stations in SWA

Figure 4.3 compares the historical distributions and the downscaled distributions for wet spell lengths at eight stations. With the possible exception of Wagin (station 29 in Figure 2.1), the downscaled distributions provide good approximations to the historical distributions, particularly for the short duration spells that encompass about 90% of wet events. Again the differences between the downscaled distributions obtained from CSIRO9 and DARLAM are slight.
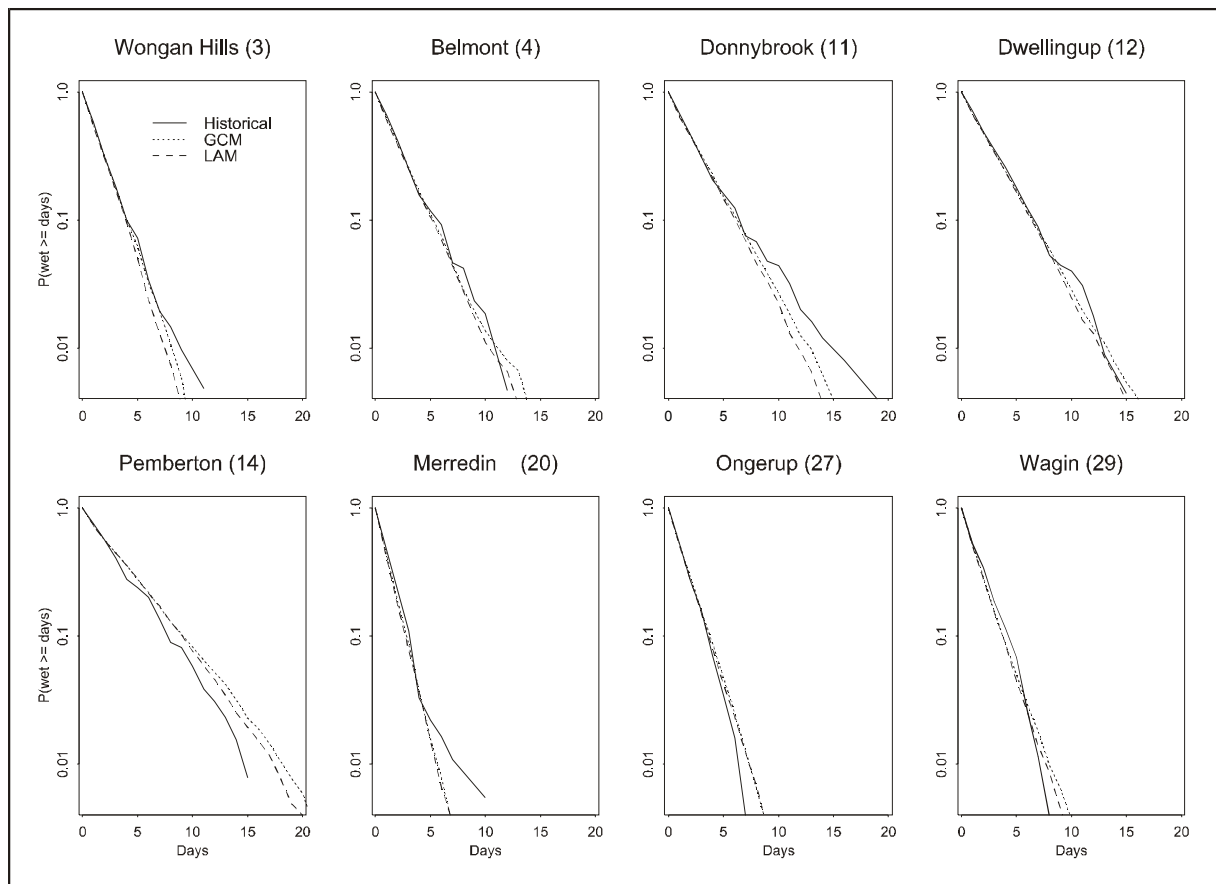
Figure 4.3   **Comparison of historical and downscaled wet spell length distributions for eight stations in SWA**

Figure 4.4 compares downscaled log-odds ratios for precipitation occurrence with historical values. The downscaled simulations clearly capture the spatial correlation between stations. There is, however, a slight bias in the ratios obtained from the downscaled LAM run.
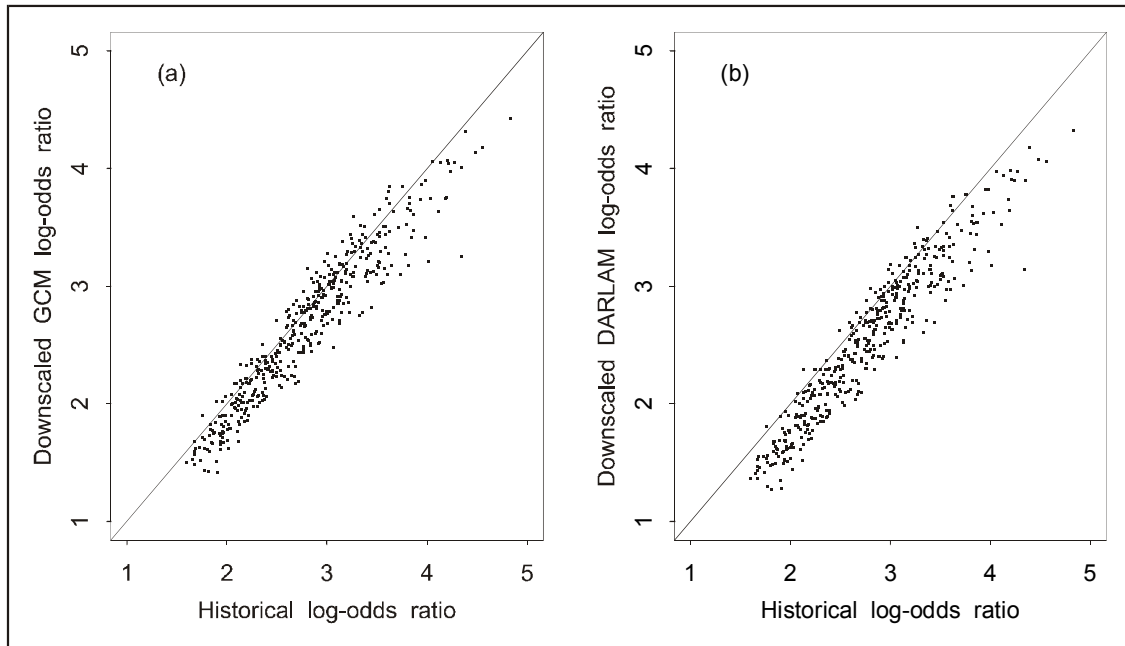
Figure 4.4　　　**Downscaled versus historical log-odds ratio**

5. CAN THE DOWNSCALING MODEL BE VALIDATED FOR CHANGED CLIMATE CONDITIONS?

5.1   Introduction

In climate change impact assessments, a fundamental caveat of downscaling methods is the presumption that the relationships between atmospheric circulation and precipitation are maintained for changed climate conditions. Many studies have shown that downscaling models fitted to historical atmospheric circulation and precipitation data are largely insensitive to changed climate conditions or inconsistent with the broad scale changes indicated by the host GCMs (e.g. Matyasovszky *et al.*, 1993a,b; Kidson & Watterson, 1995; Wilby *et al.*, 1998). Pittock (1993), Conway *et al.* (1996) and Huth (1997) warn that the relationships between circulation and local weather variables derived from historical data may be invalid for changed climate conditions. In particular, Pittock (1993) notes that global warming in climate models causes an intensification of the hydrological cycle. More recently, Wilby and Wigley (1997) state that changes in atmospheric circulation may not be enough to derive realistic simulations of precipitation for possible future climates, and that little may be achieved by the inclusion of temperature as an additional predictor in downscaling schemes. They suggest that the effect of changes in atmospheric moisture content on precipitation must be taken into account.

This section has three major objectives:

1.   to assess the potential advantages of using a set of predictors containing information about atmospheric moisture content, as well as atmospheric circulation, in a downscaling model;

2.   to determine if agreement between the daily precipitation occurrence changes indicated by LAM simulations and those obtained from downscaled LAM atmospheric fields is achievable by objective and independent means; and

3.   to develop plausible $2 \times CO_2$ scenarios for precipitation occurrence statistics at existing stations in SWA.

A feature of the study was an attempt to validate the downscaling results for $2 \times CO_2$ conditions (step 2 above). In other downscaling studies, this is usually done

informally by comparing the grid scale changes in precipitation indicated directly by a GCM with the differences between downscaled $2 \times CO_2$ and historical precipitation (e.g., Wilby *et al*., 1998). Such comparisons are based on disparate spatial scales and this makes interpretation of results difficult. In contrast, we fit *and* validate the NHMM for the LAM grid data before developing $2 \times CO_2$ scenarios for precipitation occurrence statistics at the stations. We obviously cannot *independently* validate our scenarios for $2 \times CO_2$ conditions as the behaviour of the climate system under these conditions has yet to be observed.

5.2   Approach

The study is described in detail by Charles *et al.* (1999b) so only a brief description will be given here. We used atmospheric data sets from two 10-year DARLAM simulations, one for $1 \times CO_2$ conditions (hereafter designated by LAM1) and one for $2 \times CO_2$ conditions (hereafter designated by LAM2). A climate change downscaling experiment, using the NHMM, was undertaken according to the following steps:

1.   Fit NHMMs to the LAM1 data, with the LAM1 atmospheric predictors interpolated to the grid described in Section 2. The LAM1 precipitation occurrence data were kept on the finer LAM-grid. Use both 'circulation-only' and 'circulation+moisture' sets of predictors. For each case, select the model providing distinct weather states and a reasonable compromise between the number of predictors used and the optimum BIC.

2.   Drive the selected NHMMs fitted to the LAM1 data ('circulation-only' and 'circulation+moisture' cases) with the corresponding LAM2 atmospheric predictors (also interpolated to the grid used in step 1) to generate downscaled predictions of the $2 \times CO_2$ precipitation occurrence series on the LAM-grid.

3.   Compare these downscaled $2 \times CO_2$ precipitation occurrence series with the actual LAM2 precipitation occurrence series. A favourable comparison gives us confidence that the selected NHMMs capture the modelled climate change signal.

4.   Independent of steps 1 to 3, fit NHMMs that downscale the historical atmospheric predictors (interpolated to the grid used in step 1) to the historical precipitation occurrence data for the 30 stations, again using 'circulation-only' and 'circulation+moisture' predictors. (The period from 1978 to 1987 was used to match the length of the DARLAM simulations.) Compare these selected NHMMs to those

selected in steps 1 to 3, in terms of the number of weather states and the predictors used.

5.   If the degree of agreement in step 4 is strong, use the corresponding LAM2 atmospheric predictors (again on the same grid) to drive the 'historical-fitted' NHMMs selected in step 4. This provides downscaled $2\times CO_2$ precipitation occurrence series for the 30 stations.

Steps 1 to 3 encompass the validation. We define *validity* here as the ability of a NHMM to reproduce the first order statistics of independent data (i.e. the precipitation occurrence probabilities of the LAM2 precipitation series, see step 3 above). This presumes that DARLAM provides reliable information about projected changes in rainfall at a length scale of 125 km. Secondary validation measures were the fits to the distributions of wet and dry spell lengths. We cannot validate the results from step 5, as there are no station data for $2\times CO_2$ conditions.

Box-plots of the LAM1 data and the historical data indicated that their spreads (defined by the difference of the upper and lower quartiles) and their extremes were in reasonable agreement. For the experiments presented herein, the LAM1 and historical data were centred using their respective means, and the LAM2 data were centred using the means of the LAM1 data. Thus any biases in the LAM1 means are removed before downscaling, while the $2\times CO_2$ signal ($1\times CO_2$ to $2\times CO_2$ mean shift) is retained.

5.3   Results

For the 'circulation-only' case, the best predictors for a 6-state NHMM were mean MSLP, north-south MSLP gradient and 850 hPa east-west GPH gradient (BIC = 19546).   For the 'circulation+moisture' case, the best predictors were mean MSLP, north-south MSLP gradient, and DTD (BIC = 19078).   Thus the selected NHMM for the 'circulation+moisture' case provided a better fit to the DARLAM data.

A comparison was made between the downscaled precipitation probabilities for the LAM1 'circulation-only' and 'circulation+moisture' cases with those from the LAM1 simulation. Both NHMMs provided credible reproductions of the LAM1 probabilities, with the 'circulation-only' NHMM providing a marginally better fit and the 'circulation+moisture' NHMM a small negative bias. The LAM2 precipitation probabilities are slightly smaller than those for the LAM1 simulation. The range of the percent relative differences between LAM2 and LAM1 probabilities is -12.6 to -0.12 and the median percent relative difference is -6.22. Generally, the reductions in precipitation probability increase with increasing longitude. A comparison was made between the LAM2 downscaled precipitation probabilities (obtained by driving the NHMM fitted to the LAM1 data with atmospheric data from the LAM2 run) for the 'circulation-only' and 'circulation+moisture' cases with those from the LAM2 simulation.   The downscaled precipitation probabilities for the 'circulation-only' model consistently over-estimate the LAM2 probabilities, while the 'circulation+moisture' model gives a credible reproduction of the precipitation probabilities at the DARLAM grid points. Moreover, the mean error (over the 16 DARLAM grid points that cover SWA) in the precipitation probabilities predicted by the 'circulation-only' NHMM is over four times that predicted by the 'circulation+moisture' NHMM.   Thus the 'circulation+moisture' NHMM is *validated* (in terms of the criteria set out above). The 'circulation+moisture' model was only marginally better at reproducing the dry- and wet-spell length distributions.

Comparison of the BIC values for the models fitted to the historical data for 1978 to 1987 revealed that the 'circulation-only' NHMM had a marginally lower BIC value (BIC = 36475) than the 'circulation+moisture' NHMM (BIC = 36501).   As the BIC criterion is itself an approximation, we concluded that the 'circulation+moisture' NHMM was a reasonable candidate model for the historical data. Thus there was a reasonable degree of consistency between the sets of predictors obtained from historical data and the LAM1 simulation.

Figure 5.1 shows the precipitation probabilities obtained when the fitted NHMMs are used to downscale the LAM2 atmospheric data to the 30 stations shown in Figure 2.1. The 'circulation-only' NHMM predicts slightly higher precipitation probabilities across SWA, whereas the validated 'circulation+moisture' NHMM predicts a slight decrease. The climate change signal produced by the 'circulation+moisture' NHMM is consistent with the trend indicated by the DARLAM simulations. While this result adds to our confidence in the 'circulation+moisture' NHMM, it is based on the underlying assumption that the LAM correctly simulates the climate change process.
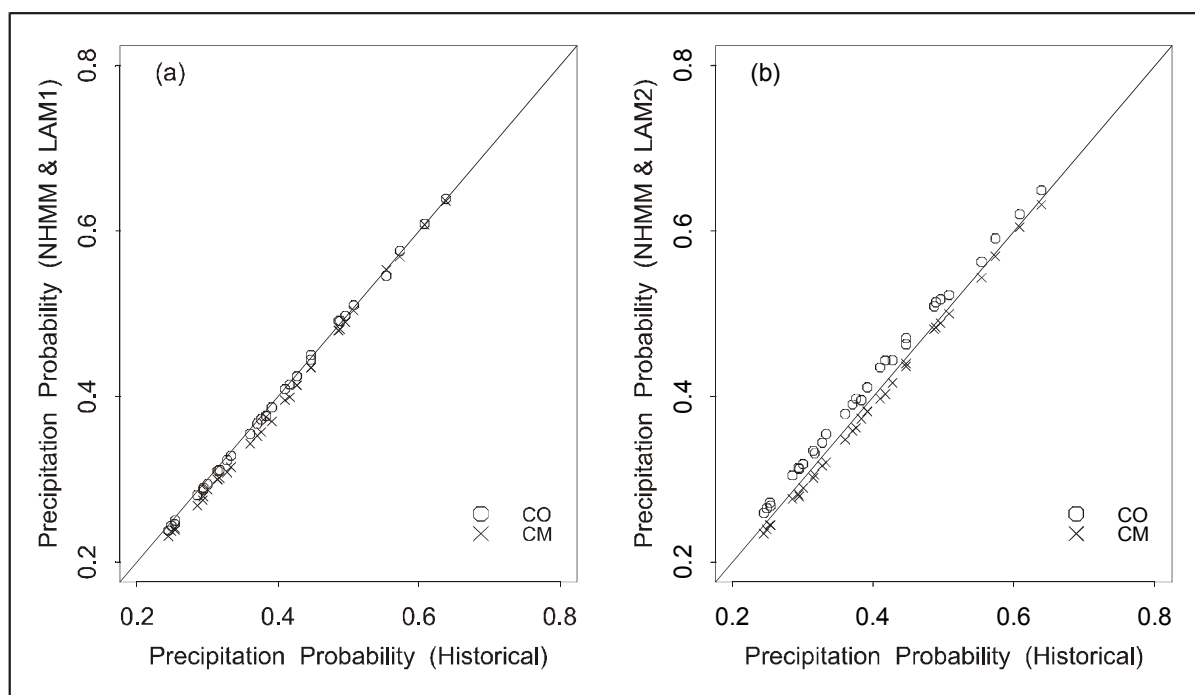
Figure 5.1   **Comparison of historical and downscaled 'winter' precipitation probabilities for 30 stations in SWA for (a) historical and (b) $2\times CO_2$ conditions**

Figure 5.2 shows the possible changes to the persistence of wet and dry spell lengths under $2\times CO_2$ conditions indicated by the 'circulation+moisture' NHMM at four stations. The elevations and precipitation at the selected stations are representative of conditions in SWA. The plots suggest little change in the short-duration spells that encompass 90% of wet and dry events. There is an overall but very slight increase in the occurrence of long-duration wet and dry spells. However, the uncertainty in the frequencies of the long-duration spells is largely due to their relatively small sample sizes within both the historical and downscaled DARLAM data.
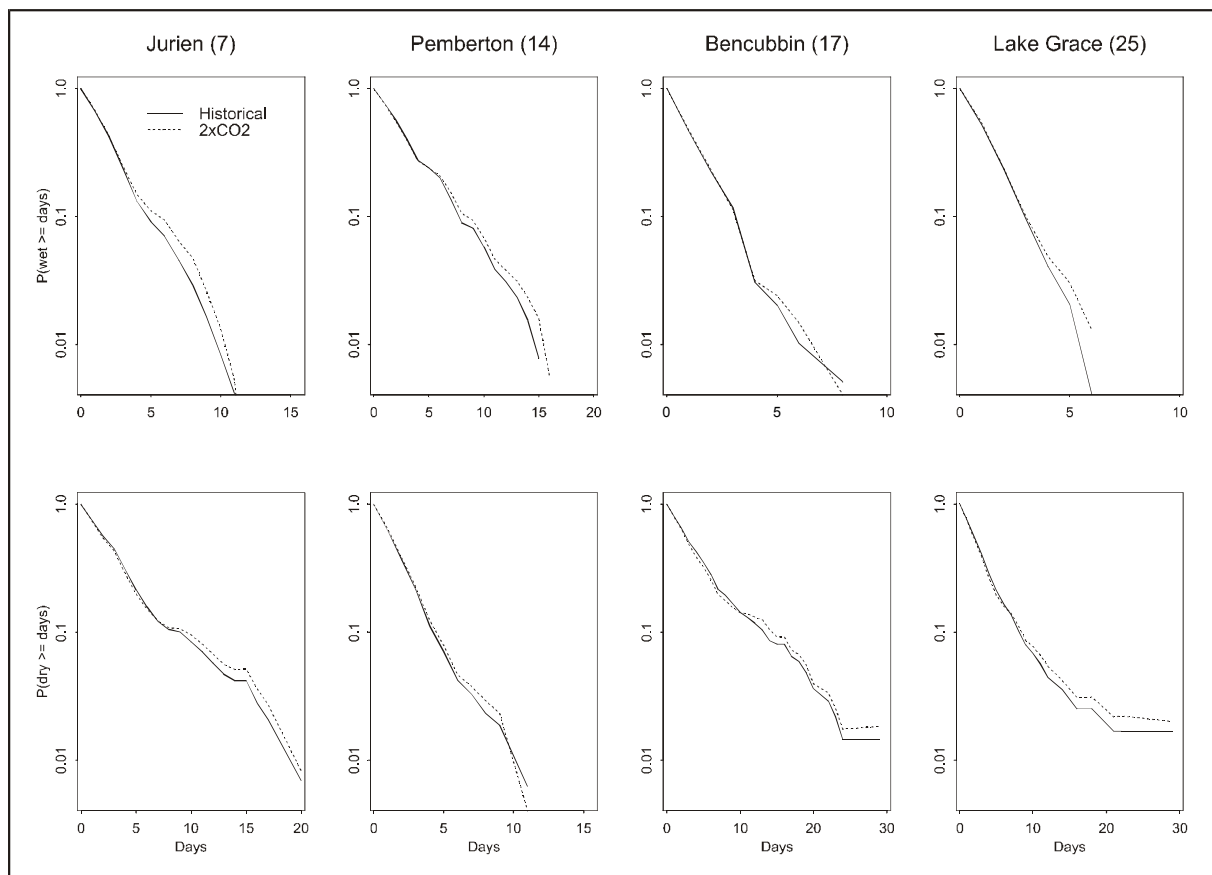
Figure 5.2   **Frequency characteristics of wet and dry spell lengths under historical (solid lines) and projected future (historical + (LAM2–LAM1)) conditions (dashed lines) for four selected stations**

Table 5.1 reports the weather state transition and steady state probabilities for the historical and downscaled LAM2 data, and indicates changes that are judged to be significant (greater than two standard errors difference) or moderate (greater than one standard error difference). The standard errors were obtained using a jackknife procedure (Efron & Tibshirani, 1993). For each data set (historical and $2\times CO_2$), each of the 10 years was successively removed from the data and the transition and steady state probabilities were recalculated. These ten sets of probabilities were then used to compute the jackknife variance. Note that this procedure does not involve refitting the NHMM for each deleted year, which would have been prohibitively expensive.

Table 5.1 Weather state transition probabilities and steady-state probabilities
for 'circulation+moisture' NHMM[#]

State	1	2	3	4	5	6
Transition Probabilities						
1	0.202	0.139	0.144	0.076	0.226	0.213
	(0.187)	(0.113)	(0.157)	(0.059)	(0.269)*	(0.215)
2	0.069	0.427	0.223	0.090	0.030	0.161
	(0.082)	(0.476)*	(0.234)	(0.072)*	(0.011)**	(0.125)*
3	0.052	0.338	0.208	0.109	0.126	0.167
	(0.065)*	(0.361)	(0.189)	(0.133)*	(0.082)**	(0.170)
4	0.023	0.210	0.214	0.247	0.205	0.101
	(0.021)	(0.158)*	(0.230)	(0.265)	(0.194)	(0.132)*
5	0.052	0.081	0.066	0.119	0.622	0.060
	(0.051)	(0.056)**	(0.051)*	(0.144)*	(0.623)	(0.075)*
6	0.031	0.045	0.101	0.209	0.432	0.182
	(0.024)	(0.030)*	(0.112)	(0.204)	(0.456)	(0.174)
Steady state probabilities						
	0.058	0.209	0.150	0.138	0.318	0.127
	(0.059)	(0.199)	(0.148)	(0.149)	(0.317)	(0.128)

[#] Figures in parentheses are downscaled probabilities for $2\times CO_2$ conditions;

* indicates changes greater than 1 standard error;

** indicates changes greater than 2 standard errors.

In Table 5.1, the steady state probabilities for States 1, 3, 5, and 6 are essentially unchanged under $2\times CO_2$ conditions. There is a marginal increase in the probability of the southwest corner of SWA being wet (State 4) and a corresponding decrease in the probability of the entire region being wet (State 2). This suggests a small decrease in the northward spread of frontal rain.

There are only a few significant changes in the transition probabilities. Consider the transitions from State 2 ('wet everywhere'). There is a significant decrease in the probability of entering State 5 ('dry everywhere') and moderate decreases in the probabilities of entering State 4 ('wet southwest corner') and State 6 ('wet south coast'). Correspondingly, there is a moderate increase in the persistence of State 2. This may indicate a decrease in the frequency of post-frontal showers. Upon leaving State 1 there is a moderate increase in the probability of entering State 5 ('dry everywhere') suggesting a reduction in the persistence of rainfall over the hinterland. State 3 ('wet west coast + central') is moderately more likely to precede State 1 ('wet hinterland') and State 4 ('wet southwest corner') with a significant decrease in the probability of entering State 5 ('dry everywhere'). The significant decrease in the probability of leaving State 5 and entering State 2, and the moderate decrease in the probability entering State 3 ('wet west coast + central'), suggests a decrease in frontal strength. This is supported by the corresponding moderate increases in the probabilities of leaving State 5 and entering States 4 and 6. The moderate decrease in the probability of leaving State 4 ('wet southwest corner') and entering State 2, and the increase in the probability of entering State 6 ('wet south coast'), indicates an increase in the tendency for rainfall in the southwest corner of SWA to contract to the south coast. This is also consistent with the suggestion of weaker frontal processes. Nevertheless, it must be emphasised that these projected changes are often for small probabilities that are based on small sample sizes (10-year LAM simulation) and thus they may confound climate change and inter-decadal climate variability.

6. WHAT IS THE POTENTIAL PREDICTABILITY OF DOWNSCALED CLIMATE MODEL SIMULATIONS?

6.1 Introduction

During Phase I of IOCI, we made an initial assessment of the predictive skill of current statistical-physical approaches to seasonal and interseasonal climate forecasting. Our aim was to ascertain the degree to which downscaled GCM runs can simulate the observed interannual variability of daily, multi-site precipitation in SWA if sea surface temperatures (SSTs) were known 'exactly' in advance.

Climate scientists often assess potential predictive skill using an ensemble of GCM simulations, where all of the simulations are forced by the same observed interannually varying SSTs but started from slightly different initial atmospheric conditions. The high computational cost of lengthy GCM runs usually constrains the ensemble size to less than 10. It is often claimed that sensitivity to initial conditions can be used to quantify the random ('chaotic') component of interannual variability, whereas the relative similarity (or lack of it) between ensemble members can be used to quantify the internal variability of the modelled climate. However, the use of different initial conditions gives insight into the effects of uncertainty in the initial state of the atmosphere only and does not acknowledge the presence of uncertainty in the parameterisations used by GCMs.

6.2 Approach

We examined the downscaled response of CSIRO9 with T63 horizontal resolution to prescribed monthly mean SSTs from 1871 to 1991. An ensemble of four climate simulations started using different initial atmospheric conditions was available for the analysis. The SSTs were obtained from an early version of the Global Sea-Ice and Sea Surface Temperature data set (GISST 1.1) prepared by the Hadley Centre of the United Kingdom Meteorological Office (UKMO). Our analyses covered the period from 1955 to 1991 as the GCM data for the preceding period (1871 to 1954) had been archived at monthly rather than daily time steps.

Given that MSLP is an important atmospheric predictor for precipitation occurrence in SWA, we used the global MSLP (GMSLP2.1) data set prepared by Hadley Centre of the UKMO (Basnett and Parker, 1997) to make a partial validation of the GCM prior to downscaling. GMSLP2.1 contains observed monthly data covering the period 1871-1994 on a $5° \times 5°$ grid.

The historical and modelled MSLPs were interpolated to the rectangular 3.75° longitudinal by 2.25° latitudinal grid described in Section 2. The validation involved comparisons of mean MSLPs for the five CSIRO9 grid points centred over SWA.

We used the extended NHMM developed by Charles *et al.* (1999a) to downscale atmospheric fields from CSIRO9. For a given GISST-CSIRO9 realisation, we generated an ensemble of 1000 realisations of the selected NHMM using the method described by Hughes and Guttorp (1994). This approach facilitates the computation of confidence levels which is essential for a meaningful assessment of skill in reproducing historical spatial and temporal patterns of interannual variability.

6.3   Results

Figure 6.1 compares monthly mean MSLP in the GMSLP2.1 data set for the 'winter' seasons in the period 1955 to 1991 with those derived from one of the GISST-CSIRO9 realisations. The historical and modelled mean MSLPs were centred using their respective 1978 to 1991 means. The unbroken curves depict smooths of the data. The smooth of the simulated post-1978 MSLPs are similar to the historical, but the smooths of the pre-1970 MSLPs are quite different. In particular, the smoothed historical MSLPs prior to 1970 are lower than their 1978 to 1991 mean whereas the smoothed modelled MSLPs for the same period are higher than their 1978 to 1991 mean. Thus there is a systematic bias in the centred GISST-CSIRO9 MSLP field during the period 1955 to about 1969. This bias was also evident in the three remaining CSIRO9 realisations. Thus downscaled simulations of precipitation are likely to be poor for the period 1955 to 1969 regardless of the realisation used.
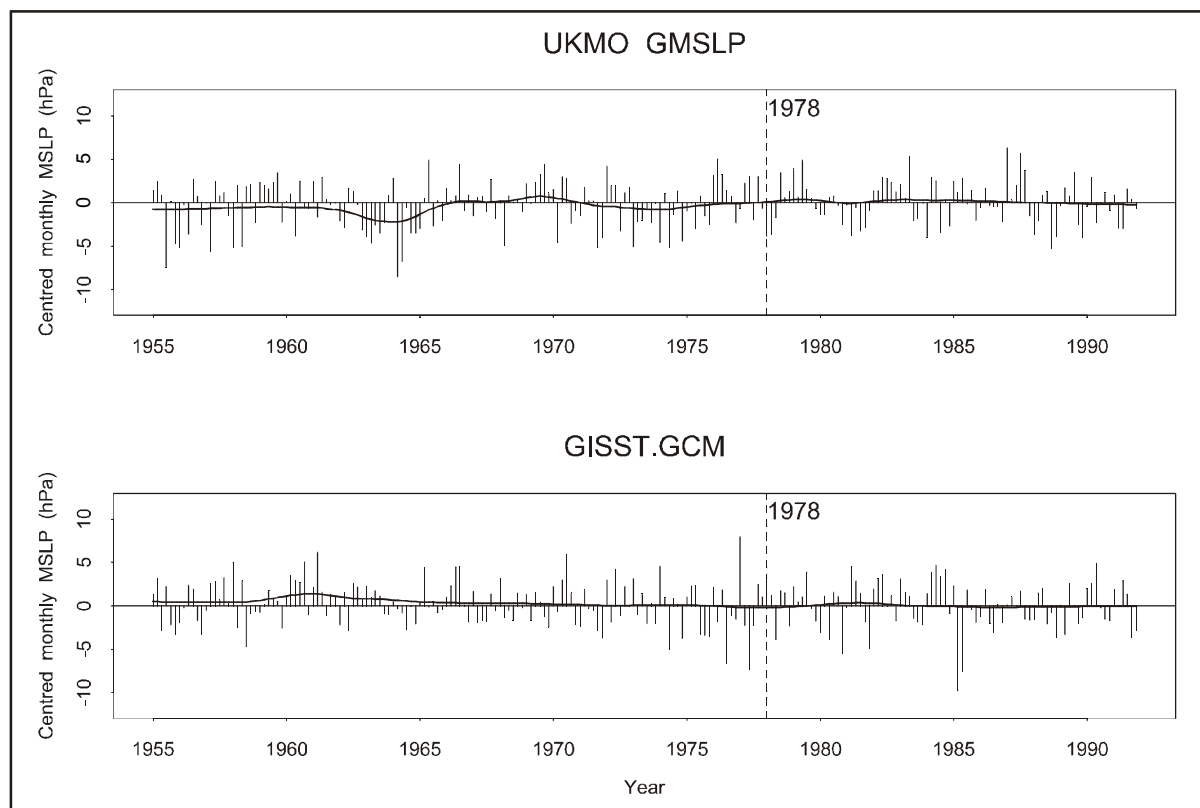
Figure 6.1   Comparison of historical and modelled centred mean MSLP fields over SWA for the period 1955 to 1991

Figure 6.2 compares the historical 'winter' precipitation series at Pemberton with the downscaled series obtained from the ensemble of 1000 realisations of the NHMM when it is driven by historical atmospheric data. The fit of the NHMM is good since the ensemble range encompasses the historical total in every year considered. However, inspection of similar plots for stations 1, 3 to 7, 12, 13 and 18 to 21 revealed that the ensemble range for 1982 did not encompass observed precipitation values. The spatial coherence of this pattern, and the observation that other (but far less severe) instances of poor fit seem to be associated with warm events in the Pacific Ocean, suggest the need for a low-frequency atmospheric predictor in the NHMM.
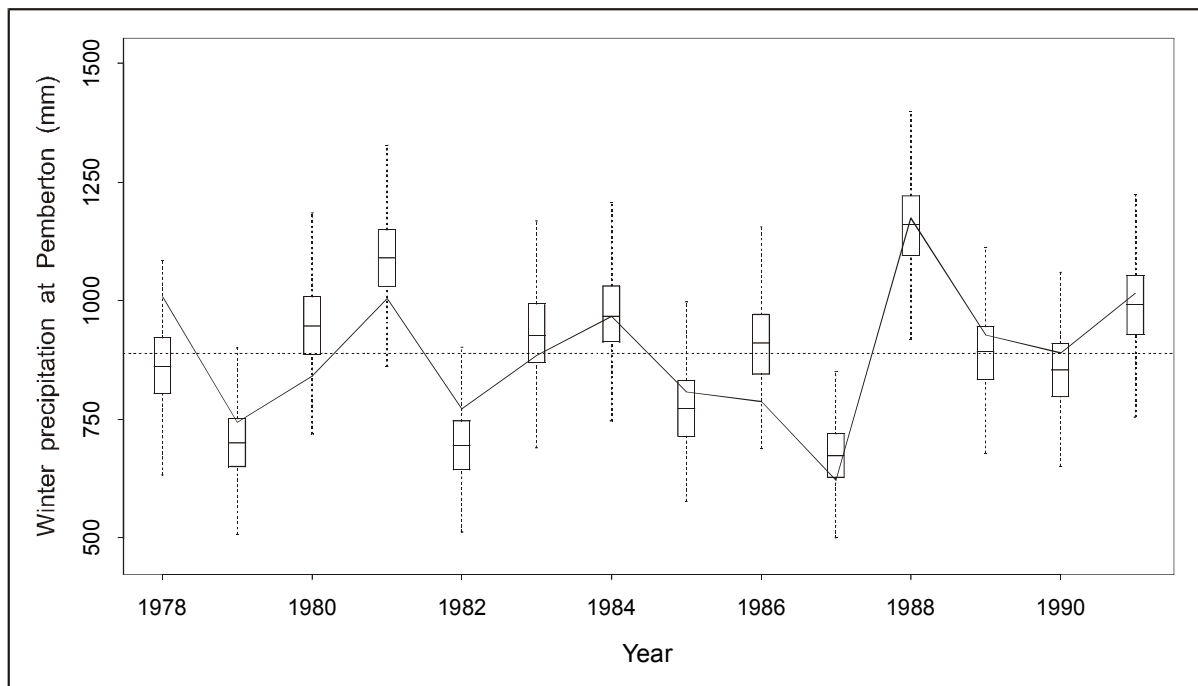
Figure 6.2 **Comparison of historical 'winter' precipitation at Pemberton (unbroken line) and boxplots of an ensemble of 1000 precipitation sequences derived from downscaled historical atmospheric fields. (A key for the interpretation of the box plots is given in the caption for Figure 3.2)**

Figure 6.3 compares the historical 'winter' precipitation series at Pemberton with the series obtained from the downscaled GISST-CSIRO9 run corresponding to the 'winter' MSLP series depicted in Figure 6.1. Apart from the poor simulation for 1984, the simulations for 1970 to 1991 are of a reasonable standard. However, simulated precipitation for 1955 to 1969 consistently falls below the observed. This is consistent with the direction of the bias in the GISST-CSIRO9 MSLPs for the same period.
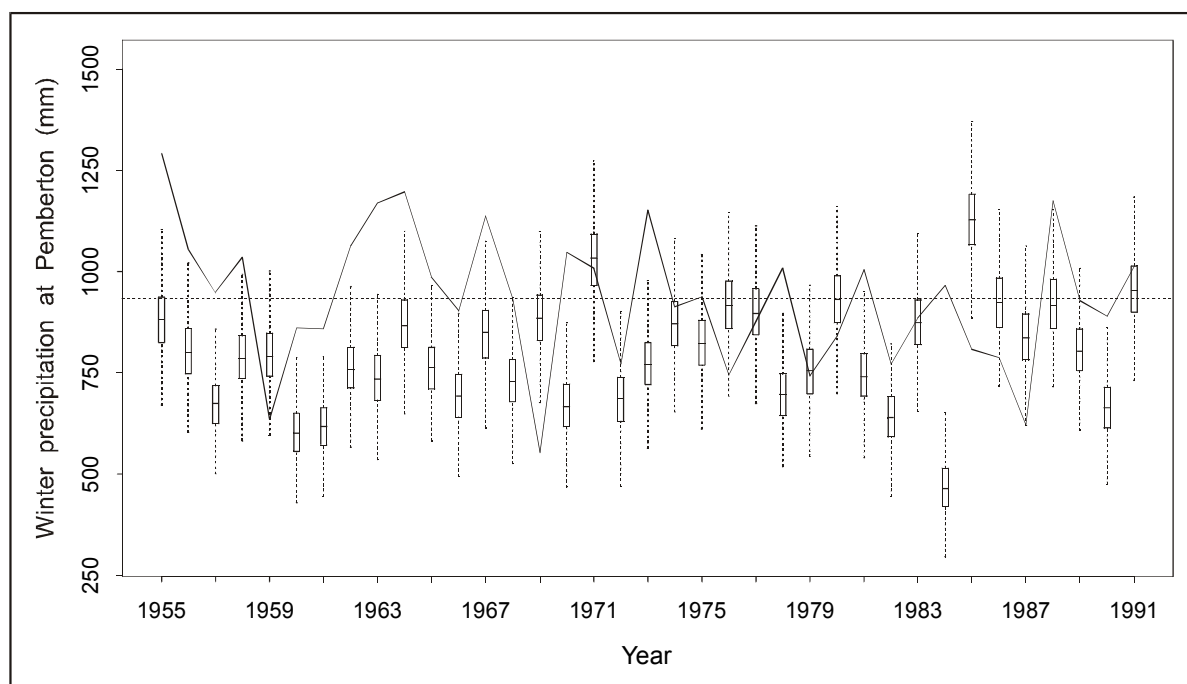
Figure 6.3   **Comparison of historical 'winter' precipitation at Pemberton (unbroken line) and an ensemble of 1000 precipitation sequences derived from a downscaled GISST-forced CSIRO9 run (box plots). (A key for the interpretation of box plots is given in the caption for Figure 3.2)**

Although the results for the GISST-CSIRO9 runs were mixed, three factors suggest that this may be due to erroneous pre-1970 SSTs in the GISST 1.1 data set rather than deficiencies in CSIRO9 or the NHMM: (1) the similarity of historical and modelled MSLP fields for the period 1978 to 1991; (2) the concurrence of this period with the reliable observation of SSTs by satellites; and (3) the consistency of the systematic bias in the modelled MSLP fields across the four GISST-CSIRO9 realisations for years prior to 1970.

7.   CONCLUSIONS

7.1   Summary of the Investigation

Our downscaling experiments for the Indian Ocean Climate Initiative (IOCI) have focused on the application of an extended nonhomogeneous hidden Markov model (NHMM) to daily 'winter' (May to October) precipitation across a network of 30 stations scattered throughout south-west Western Australia (SWA).   This model was selected on the basis of its documented performance, generality, and ability to cope with small nonstationarity in atmospheric data. We have addressed the following questions:

1.   Can we downscale observed atmospheric fields for SWA?

2.   Are downscaled climate model simulations for SWA representative of present day conditions?

3.   Can we validate a downscaling model for changed climate conditions?

4.   What is the potential predictability of downscaled climate model simulations for SWA?

Our main findings are as follows:

1.   When fitted to and driven by historical atmospheric circulation data for SWA, the NHMM accurately simulates the wet-day probabilities, the frequency characteristics of dry- and wet-spell lengths, the daily precipitation amount distributions at each station, and the inter-site correlations for daily precipitation amounts over the 15 year period from 1978 to 1992. This period corresponded to the length of the Bureau of Meteorology's upper air archive when the NHMM was first applied to SWA. Examination of precipitation amount statistics indicates that the NHMM provides a simple and parsimonious method of simulating daily precipitation amounts and their local spatial dependencies in the network. Nevertheless, there is scope for refinement of precipitation amount simulation.

2.   Downscaled simulations from either the CSIRO general circulation model (CSIRO9) or the CSIRO limited area model (DARLAM) reproduce observed precipitation probabilities and dry- and wet-spell frequencies at the 30 precipitation stations in

SWA. In contrast, the CSIRO9 and DARLAM simulations of precipitation tend to under-estimate the frequency of dry spells and over-estimate the probability of precipitation and the frequency of wet spells.

3. The NHMM provides a credible downscaling technique for assessing climate change in SWA provided a variable characterising the closeness of the atmosphere to saturation rather than absolute moisture content is included in the predictor set. The inclusion of this predictor (850 hPa dew point temperature depression) was found to be defensible when the NHMM was fitted to either modelled or historical data. Driving the NHMM fitted to historical data with modelled atmospheric fields for changed climate ($2 \times CO_2$) conditions results in a small decrease in the probability of precipitation across SWA and a small change in the region's synoptic climatology. This result is based on only one 10-year LAM simulation and is only relevant to the case study region. However, our results demonstrate that the validation of a statistical downscaling technique for present day conditions does not necessarily imply legitimacy for changed climate conditions. Thus statistical downscaling studies that have not attempted to determine the plausibility of their predictions for the changed climate conditions should be viewed with caution.

4. Downscaled simulations from an ensemble of four CSIRO9 runs forced by historical sea surface temperatures (SSTs) failed to reproduce the year-to-year variations in 'winter' precipitation for the period 1955 to late 1960s. However, reasonable simulations were obtained for 1970 to 1991. Thus the potential predictability of downscaled CSIRO9 simulations was found to be reasonable for this period. Comparison of CSIRO9 and historical mean sea level pressure (MSLP) fields suggested that the poor results for the 1950s to 1960s were due largely to errors in the historical SST data rather than the presence of random effects or systematic error in either CSIRO9 or the NHMM.

5. Overall, the above results indicate that CSIRO9 and DARLAM produce credible simulations of historical atmospheric circulation patterns over SWA. If this were not the case, the statistics of the downscaled simulations would have borne little resemblance to the observed.

7.2   Future Research

Our proposed research plan for Phase 3 of IOCI is as follows:

1.   The development of a new NHMM framework that considers precipitation amounts and occurrences jointly.

2.   Investigation of the stationarity of NHMM parameters using global MSLP data sets.

3.   Driving the NHMM with global MSLP data sets to obtain insight into the long-term, temporal and spatial changes in historical synoptic patterns over SWA.

4.   Investigation of the relationship between the changes in synoptic patterns over time and the observed secular breaks in SWA precipitation.

5.   A new study of potential predictability using the new NHMM, the Mark 3 version of the CSIRO GCM and an updated historical SST data set.

6.   For GCM grid cells around SWA, investigation of the interdecadal variability in a 1000-year GCM run with a view to detecting any secular changes in modelled atmospheric series and downscaled precipitation series and identifying their causes.

Outcomes from this work will include:

1.   Further insight into the causes and characteristics of the secular breaks in SWA precipitation series at interannual to decadal time scales. Unlike univariate time series analyses, the breaks will be identified in space-time rather than time alone. Also, the NHMM provides a natural framework for assessing these breaks in terms of changes in atmospheric circulation indices that directly influence precipitation occurrence and amount.

2.   Assessment of potential interseasonal climate forecasting skill at local and regional scales. This will quantify the skill of statistical-physical forecasts when given accurate sea surface temperature forecasts.

3.   Frequency characteristics of precipitation (occurrence and amount), and the frequency-intensity-duration characteristics of wet- and dry-spells, at interannual to centennial time scales.

4.   An ensemble of millennial daily precipitation series for climate impacts modelling by state agencies.

5.   A new synoptic classification for SWA based on the spatial patterns of precipitation occurrence.

Our proposed research linkages are:

1.   *CSIRO Atmospheric Research* – 1,000-year CSIRO9 Mark 2 GCM run; and an ensemble of ten GISST4-forced CSIRO Mark 3 GCM runs (to be carried out by Queensland Department of Natural Resources).

2.   *Bureau of Meteorology (Research Centre and Perth Regional Office)* – comparison of secular breaks in spatial patterns of rainfall occurrence with the Bureau's previous work on changes in atmospheric circulation; and meteorological advice on the selection of candidate atmospheric predictors for the NHMM.

3.   *University of Washington, Seattle* – development and testing of a new NHMM that considers precipitation occurrences and amounts jointly.

4.   *CSIRO Mathematical and Information Sciences* – advice on advanced statistical issues and insights into key atmospheric predictors.

8. REFERENCES

Arnell, N., Bates, B.C., Lang, H. Magnuson, J.J., and Mulholland, P. (1996). Hydrology and freshwater ecology. In: *Climate Change 1995: Impacts, Adaptations and Mitigation of Climate Change: Scientific-Technical Analyses.* Contribution of Working Group II to the Second Assessment Report of the Intergovernmental Panel on Climate Change. R.T. Watson, M.C. Zinyowera, and R.H. Moss (ed.), Cambridge Univ. Press, Cambridge, 325-363.

Bardossy, A. and Plate, E.J. (1991). Modelling daily rainfall using a semi-Markov representation of circulation pattern occurrence. *J. Hydrol.*, 122, 33-47.

Bardossy, A. and Plate, E.J. (1992). Space-time model for daily rainfall using atmospheric circulation patterns. *Water Resour. Res., 28*(5), 1247-1259.

Bartholy, J., Bogardi, I. and Matyasovszky, I. (1995). Effect of climate change on regional precipitation in Lake Balaton watershed. *Theor. Appl. Climatol., 51*, 237-250.

Basnett, T.A. and Parker, D.E. (1997). Development of the global mean sea level pressure data set GMSLP2. *Hadley Centre for Climate Prediction and Research, U.K. Meteorological Office, Climate Res. Tech. Note No. 79*, 60 pp.

Bates, B.C., Charles, S.P. and Hughes, J.P. (1998). Stochastic downscaling of numerical climate model simulations. *Environ. Model. & Software, 13*(3-4), 325-331.

Bates, B.C., Charles, S.P. and Hughes, J.P. (1999). Stochastic downscaling of GCM simulations. In: *Applications of Seasonal Climate Forecasting in Agricultural and Natural Ecosystems – The Australian Experience.* G. Hammer and C.J. Mitchell (ed.), Kluwer Academic Publishers, (accepted 25 June 1998).

Bogardi, I., Matyasovszky, I., Bardossy, A., and Duckstein, L. (1993). Application of a space-time stochastic model for daily precipitation using atmospheric circulation patterns. *J. Geophys. Res.*, *98*(D9), 16,653-16,667.

Charles, S.P., Hughes, J.P., Bates, B.C., and Lyons, T.J. (1996). Assessing downscaling models for atmospheric circulation - local precipitation linkage. Proc. Int. Conf.

Water Resour. and Environ. Res.: Towards the 21st Century. October 29-31, 1996, Water Resources Research Center, Kyoto University, Japan, Vol. 1, 269-276.

Charles, S.P., Bates, B.C. and Hughes, J.P. (1999a). A spatio-temporal model for downscaling precipitation occurrence and amounts. *J. Geophys. Res., D,* (accepted 23 February 1999).

Charles, S.P., Bates, B.C., Whetton, P.H., and Hughes, J.P. (1999b). Validation of a downscaling model for changed climate conditions in southwestern Australia. *Clim. Res., 12*(1), 1-14.

Crane, R.G. and Hewitson, B.C. (1998). Doubled CO_2 precipitation changes for the Susquehanna basin: down-scaling from the GENESIS general circulation model. *Int J Climatol., 18*, 65-76.

Conway D., Wilby, R.L., Jones, P.D. (1996). Precipitation and airflow indices over the British Isles. *Clim Res 7*, 169-183.

Efron, B. and Tibshirani, R.J. (1993). *An Introduction to the Bootstrap.* Chapman and Hall, New York, 450 pp.

Enke, W. and Spekat, A. (1997). Downscaling climate model outputs into local and regional weather elements by classification and regression. *Clim. Res., 8*, 195-207.

Gates, W.L., Henderson-Sellers, A., Boer, G.J., Folland, C.K., Kitoh, A., McAvaney, B.J., Semazzi, F., Smith, N., Weaver, A.J., and Zeng, Q.-C. (1996). Climate models - evaluation. In: *Climate Change 1995: The Science of Climate Change.* Contribution of Working Group I to the Second Assessment Report of the Intergovernmental Panel on Climate Change, J.T. Houghton, L.G. Meira Filho, B.A. Callander, N. Harris, A. Kattenberg, and K. Maskell (ed.), Cambridge Univ. Press, Cambridge, 229-284.

Gentilli, J. (1972). *Australian Climate Patterns*. Nelson, Melbourne, 285 pp.

Hughes, J.P. and Guttorp, P. (1994). A class of stochastic models for relating synoptic atmospheric patterns to regional hydrologic phenomena. *Water Resour. Res., 30*(5), 1535-1546.

Hughes, J.P., Guttorp, P. and Charles, S.P. (1999). A non-homogeneous hidden Markov model for precipitation occurrence. *Appl. Statist.*, *48* (1), 15-30.

Huth, R. (1997). Potential of continental-scale circulation for the determination of local daily surface variables. *Theor Appl Climatol., 56*, 165-186.

Kotz, S. and Johnson, N.L. (1985). *Encyclopedia of Statistical Sciences*, Vol. 6, John Wiley and Sons, New York, 758 pp.

Kidson, J.W. and Watterson, I.G. (1995). A synoptic climatological evaluation of the changes in the CSIRO nine-level model with doubled CO_2 in the New Zealand region. *Int. J. Climatol., 15,* 1179-1194.

Matyasovszky, I., Bogardi, I., Bardossy, A., and Duckstein, L. (1993a). Estimation of local precipitation statistics reflecting climate change. *Water Resour. Res., 29*(12), 3955-3968.

Matyasovszky, I., Bogardi, I., Bardossy, A., and Duckstein, L. (1993b). Space-time precipitation reflecting climate change. *Hydrol. Sci. J., 38*(6), 539-558.

McGregor, J.L. (1997). Regional climate modelling. *Meteorol. Atmos. Phys., 63*, 105-117.

McGregor, J.L., Gordon, H.B., Watterson, I.G., Dix, M.R., and Rotstayn, L.D. (1993). The CSIRO 9-level atmospheric general circulation model. *CSIRO Div. Atmos. Res. Tech. Paper No. 26*, 89 pp.

Mearns, L.O., Giorgi, F., McDaniel, L., & Shields, C. (1995). Analysis of daily variability of precipitation in a nested regional climate model: comparison with observations and doubled CO_2 results. *Glob. Planet. Change , 10*, 55-78.

Pittock, A.B. (1993). Climate scenario development. In: *Modelling Change in Environmental Systems*. A.J. Jakeman, M.B. Beck and M.J. McAleer (ed.), John Wiley and Sons, New York, 481-503

Walsh, K.J.E. and McGregor, J.L. (1995). January and July climate simulations over the Australian region using a limited-area model. *J. Clim., 8*(10), 2387-2403.

Walsh, K.J.E. and McGregor, J.L. (1997). An assessment of simulations of climate variability over Australia with a limited area model. *Int. J. Climatol.*, *17*, 201-223.

Whetton, P., Pittock, A.B., Labraga, J.C., Mullan, A.B., and Joubert, A. (1996). Southern hemisphere climate: Comparing models with reality. In: *Climate Change: Developing Southern Hemisphere Perspectives*. T.W. Giambelluca and A. Henderson-Sellers (ed.), John Wiley and Sons, New York, 89-130.

Wilby, R.L. and Wigley, T.M.L. (1997). Downscaling general circulation model output: a review of methods and limitations. *Prog Phys Geog 21*(4), 530-548.

Wilby, R.L., Hassan, H. and Hanaki, K. (1998). Statistical downscaling of hydrometeorological variables using general circulation model output. *J. Hydrol.*, *205*, 1-19.

Wright, P.B. (1974). Seasonal rainfall in southwestern Australia and the general circulation. *Mon. Weather Rev.*, *102*, 219-232.

Zorita, E., Hughes, J.P., Lettenmaier, D.P., and Von Storch, H. (1995). Stochastic characterization of regional circulation patterns for climate model diagnosis and estimation of local precipitation. *J. Climate, 8*, 1023-1042.

APPENDIX A – GLOSSARY

General circulation	The global-scale wind system that largely determines the broad climate patterns on Earth.
Dew point temperature	Temperature to which air needs to be cooled for condensation to occur at a given atmospheric pressure and mixing ratio.
Diurnal	Relates to actions or events that occur during a 24-hour cycle or recurs every 24 hours.
Downscaling	Quantification of the relation of local- and regional-scale climate variables to larger scale atmospheric patterns. These patterns may be observed or simulated by dynamical climate models.
Dry spell	A sequence of consecutive days during which daily precipitation remains below 0.3 mm.
Equilibrium run	An experiment with a numerical climate model where a step change in atmospheric CO_2 concentration is applied and the model is allowed to attain a new equilibrium. These runs do not provide information about the effects of transient changes in CO_2 on the climate system.
Front	The transition zone or interface between two air masses of contrasting wind, temperature and density.
Geopotential height	The work that must be done against gravity to raise a mass of 1 kg from sea-level to the level of interest in the atmosphere.
Markov process	A stochastic process in which the 'future' is determined by the 'present' and is independent of the 'past'.
Mean Sea Level Pressure	Total atmospheric pressure at the average height of the sea for all tidal stages over a 19-year period.

Mixing ratio	Ratio of the mass of water vapour to the mass of dry air in a given volume of air.
Precipitation	Any and all forms of water that falls from clouds and reaches the earth's surface.
Quantile	The value of a variable below which a certain proportion of the variable values will fall.
Ridge	An elongated area of high atmospheric pressure that is associated with an area of maximum anticyclonic circulation. (An anticyclone is also known as a area of high atmospheric pressure.)
Trough	An elongated area of low atmospheric pressure that is associated with an area of minimum cyclonic circulation.
Wet spell	A sequence of consecutive days during which daily precipitation equals or exceeds 0.3 mm.

APPENDIX B – LIST OF ACRONYMS

BIC   Bayesian Information Criterion.

CLW   CSIRO Land and Water.

DARLAM   Limited area model developed by CSIRO Atmospheric Research.

DTD   Dew point temperature depression.

GCM   General circulation model.

GISST   Global Sea-Ice and Sea Surface Temperature data set prepared by the Hadley
            Centre of the United Kingdom Meteorological Office.

GMT   Greenwich Mean Time: the 24-hour time scale used throughout the scientific
            and military communities.   Other names for this time measurement are
            Universal Time Coordinate (UTC) and Zulu (Z).

GPH   Geopotential height.

CSIRO9   Spectral 9-level general circulation model developed by CSIRO Atmospheric
            Research.

IOCI   Indian Ocean Climate Initiative.

LAM   Limited area model.

MSLP   Mean sea level pressure.

NHMM   Nonhomogeneous hidden Markov model.

SST   Sea surface temperature.

SWA   South-west Western Australia.

UKMO   United Kingdom Meteorological Office.